

Weighted-Graph-Based Change Point Detection

Lizhen Nie and Dan L. Nicolae *

November 30, 2021

Abstract

We consider the detection and localization of change points in the distribution of an offline sequence of observations. Based on a nonparametric framework that uses a similarity graph among observations, we propose new test statistics when at most one change point occurs and generalize them to multiple change points settings. The proposed statistics leverage edge weight information in the graphs, exhibiting substantial improvements in testing power and localization accuracy in simulations. We derive the null limiting distribution, provide accurate analytic approximations to control type I error, and establish theoretical guarantees on the power consistency under contiguous alternatives for the one change point setting, as well as the minimax localization rate. In the multiple change points setting, the asymptotic correctness of the number and location of change points are also guaranteed. The methods are illustrated on the MIT proximity network data.

**Department of Statistics, University of Chicago*

1 Introduction

The task of change point detection (CPD) is to identify possible changes in the distribution of a time-ordered sequence. Classical change point detection methods assume parametric models or are focused on univariate settings. Novel approaches are needed due to the increasing richness of high-dimensional and non-Euclidean data in various scientific applications. For instance, identifying changes in genetic networks involves graphical encoding of data (Li et al., 2011; Lu et al., 2011). In financial modeling, segmentation of historical data involves multidimensional correlated assets (Talih and Hengartner, 2005).

The change point problem is usually decomposed into two stages: detection (testing for whether the distribution changes); and localization (estimation of the location of change point(s) when detected). Thus, an ideal change point method should have (1) high power for detection, and (2) high accuracy in localization.

Recently, several nonparametric change point methods have been proposed. They can be classified into three main categories: kernel-based (Arlot et al., 2019; Celisse et al., 2018; Chang et al., 2019; Desobry et al., 2005; Garreau et al., 2018; Harchaoui et al., 2009,?; Huang et al., 2014; Li et al., 2015), Euclidean-distance-based (Matteson and James, 2014), and graph-based (Chen, 2019; Chen et al., 2019, 2018; Chen and Friedman, 2017; Chen et al., 2015; Chu and Chen, 2018; Chu et al., 2019; Liu and Chen, 2020; Song and Chen, 2020). Kernel-based methods are applicable to any type of data, but existing ones either do not offer false positive controls (Arlot et al., 2019; Celisse et al., 2018; Desobry et al., 2005; Garreau et al., 2018), or do not provide guarantees on localization accuracy (Chang et al., 2019; Desobry et al., 2005; Harchaoui et al., 2009,?; Huang et al., 2014; Li et al., 2015). Euclidean-distance-based methods (Matteson and James, 2014) provide localization consistency, but they are not applicable to non-Euclidean data. Graph-based methods Chen et al. (2015) are built on a binary similarity graph among observations. They are applicable to any type of data and yield analytic formulas for controlling type I error. However, they do not provide theoretical guarantees on testing power or localization consistency, and using binary graphs leads to information loss.

Our work is based on the graph-based change point detection framework but utilizes the weight information in the graph. We consider both settings where at most one change point (AMOC) exists or multiple change points are possible. Starting with the AMOC setting, we propose new statistics and give explicit formulas for type I error control. Further, we show that the proposed tests are consistent under local alternatives and the estimated change point has the minimax localization rate. A generalized algorithm for multiple change points setting is also proposed, and is guaranteed to identify both the correct number and locations of change points. Our framework unifies the kernel-based, Euclidean-distance-based and graph-based CPD methods, leading to a general CUSUM-type [Page \(1954\)](#) decomposition of the proposed statistics which holds for any distance and any data under mild assumptions, and providing a better understanding of properties of the proposed statistics.

This paper is structured as follows: Section 2 introduces problem setting and background, Section 3 proposes new statistics and discusses its connection to previous methods, Section 4 presents the asymptotic theoretical results, Section 5 shows simulation results, Section 6 shows results on a real data example, Section 7 gives discussion and conclusions.

2 Preliminary Setups

2.1 Problem Setting

Suppose we observe an independent, time-ordered sequence $\{y_i\}_{i=1}^n$. Depending on the number of change points, we consider two settings in increasing complexity.

At most one change point (AMOC) In the simplest setting, there exists at most one change point. Suppose $F_0 \neq F_1$ are probability distributions on the space y_i 's take values. We are concerned with the following problems:

1. (Detection) Testing the null hypothesis

$$H_0 : y_i \sim F_0, i = 1, 2, \dots, n$$

against the single change-point alternative

$$H_A : \exists \rho^* \in (0, 1) \text{ s.t. } \begin{cases} y_1, \dots, y_{\tau^*} \sim F_0 \\ y_{\tau^*+1}, \dots, y_n \sim F_1, \end{cases}$$

where $\tau^* = \lceil n\rho^* \rceil$. Here $\lceil x \rceil$ denotes the least integer no less than x .

2. (Localization) When rejecting H_0 , obtain an estimator $\hat{\tau}$ of the true change point location.

Multiple change points In this setting, there is a fixed but unknown number K of change points that partition the whole sequence into $K + 1$ phases. The change points are $\mathcal{D} = \{\tau_1^*, \tau_2^*, \dots, \tau_K^*\}$ where $0 < \rho_1^* < \rho_2^* < \dots < \rho_K^* < 1$, $\tau_k^* = \lceil n\rho_k^* \rceil$. Suppose

$$y_{\tau_k^*+1}, y_{\tau_k^*+2}, \dots, y_{\tau_{k+1}^*} \sim F_k,$$

where $F_k \neq F_{k+1}$ for all $k = 0, 1, \dots, K$, $\tau_0^* := 0$ and $\tau_{K+1}^* := n$. When there are no change points, $K = 0$, $\mathcal{D} = \emptyset$. Our task is to estimate K as well as \mathcal{D} .

2.2 Graph-based Methods

The cornerstone of this paper is the graph-based CPD framework (Chen et al., 2018; Chen and Friedman, 2017; Chen et al., 2015; Chu et al., 2019). This section introduces important ideas and quantities behind them.

Graph-based CPD methods focus on the AMOC setting. They are based on binary similarity graphs where nodes represent observations and edges similarity. A binary similarity graph is usually constructed from a weighted one via a minimum spanning tree (MST) (Friedman and Rafsky, 1979), minimum distance pairing (Rosenbaum, 2005) or nearest neighbor (Henze, 1988). For each t , denote the count of edges among $\{y_i\}_{i=1}^t$ (phase I) by $C_{B_1(t)}$ and that among $\{y_i\}_{i=t+1}^n$ (phase II) by $C_{B_2(t)}$. Utilizing $C_{B_1(t)}$ and $C_{B_2(t)}$, various scan statistics have been proposed, which are found to be combinations of two statistics:

$$Z_w(t) = \text{Strd} \left(\frac{n-t-1}{n-2} C_{B_1(t)} + \frac{t-1}{n-2} C_{B_2(t)} \right), \quad (1)$$

$$Z_{\text{diff}}(t) = \text{Strd} (C_{B_1(t)} - C_{B_2(t)}), \quad (2)$$

where Strd denotes a standardized statistic such that it has the same variance and mean across t . For example, the generalized edge-count two-sample test statistic G in [Chen and Friedman \(2017\)](#) can be written as

$$G := \max_t G(t) \quad \text{where} \quad G(t) := (Z_w(t))^2 + (Z_{\text{diff}}(t))^2,$$

and the max-type edge-count test statistic M from [Chu et al. \(2019\)](#) is defined as

$$M := \max_t M(t) \quad \text{where} \quad M(t) := \max(Z_w(t), |Z_{\text{diff}}(t)|).$$

A change point is detected when G (or M) exceeds a given threshold, and its estimated location is defined as $\hat{\tau} = \arg \max_t G(t)$ (or $\hat{\tau} = \arg \max_t M(t)$).

Further, [Chu et al. \(2019\)](#) found that $Z_w(t)$ works well for detecting mean changes, and $Z_{\text{diff}}(t)$ for detecting scale changes. Some intuition: for mean change, observations from the same distribution are similar to each other, and thus edges are more likely to form among them. In this case the true change point τ^* is the time t which maximizes the number of edges within $\{y_i\}_{i=1}^t$, $C_{B_1(t)}$, and within $\{y_i\}_{i=t+1}^n$, $C_{B_2(t)}$. The weights in $Z_w(t)$ balance the influence from the unequal sample size of $\{y_i\}_{i=1}^t$ and $\{y_i\}_{i=t+1}^n$. For scale changes, edges are more likely to form among observations from the distribution with smaller dispersion. There the true change point τ^* is the time t maximizing the difference between number of edges within $\{y_i\}_{i=1}^t$ and that within $\{y_i\}_{i=t+1}^n$, i.e., $|C_{B_1(t)} - C_{B_2(t)}|$, which is $|Z_{\text{diff}}(t)|$.

2.3 Notations

We denote $[n] = \{1, 2, \dots, n\}$, $A(t) = \{(i, j) \in [n]^2 : i \leq t, j > t\}$, $B_1(t) = \{(i, j) \in [n]^2 : i \leq t, j \leq t, i \neq j\}$ and $B_2(t) = \{(i, j) \in [n]^2 : i > t, j > t, i \neq j\}$. Similarly, we denote $A^{l,r}(t) = \{(i, j) \in [n]^2 : l \leq i \leq t, t < j \leq r\}$, $B_1^{l,r}(t) = \{(i, j) \in [n]^2 : l \leq i \leq t, l \leq j \leq t, i \neq j\}$ and $B_2^{l,r}(t) = \{(i, j) \in [n]^2 : t < i \leq r, t < j \leq r, i \neq j\}$. For any set $D \subseteq [n]^2$, we denote $d_D = \sum_{(i,j) \in D} d(y_i, y_j)$ and $\bar{d}_D = \sum_{(i,j) \in D} d(y_i, y_j) / |D|$ where $|D|$ is the cardinality of D . We write $\bar{y} = \frac{1}{n} \sum_{i=1}^n y_i$. For any function f , we write $\bar{f}(y)_{t-} = \frac{1}{t} \sum_{i=1}^t f(y_i)$, $\bar{f}(y)_{t+} = \frac{1}{n-t} \sum_{i=t+1}^n f(y_i)$. Denote $V(f(y), \|\cdot\|)_{t-} = \frac{1}{t-1} \sum_{i=1}^t \|f(y_i) - \bar{f}(y)_{t-}\|^2$ and

$V(f(y), \|\cdot\|)_{t+} = \frac{1}{n-t-1} \sum_{i=t+1}^n \|f(y_i) - \bar{f}(y)_{t+}\|^2$, which can be viewed as the estimated dispersion of $f(y)$ in phase I or II measured in $\|\cdot\|$. We denote \xrightarrow{w} as weak convergence, \mathcal{O}_p stochastic as boundedness, and o_p as convergence in probability. Denote W^0 as Brownian bridge.

3 Proposed statistics

Using unweighted graphs ultimately leads to information loss, motivating the development of weighted-graph-based change point detection methods. Suppose we have an weighted undirected graph on $\{y_i\}_{i=1}^n$ where an edge between y_i and y_j comes with a weight $d(y_i, y_j)$ and d is a given distance. For each t , the $n(n-1)/2$ pairs of weights can be split into three parts: $d_{B_1(t)}$ which corresponds to sum of distances within $\{y_i\}_{i=1}^t$, $d_{B_2(t)}$ which corresponds to sum of distances within $\{y_i\}_{i=t+1}^n$, and $d_{A(t)}$ which corresponds to sum of distances between $\{y_i\}_{i=1}^t$ and $\{y_i\}_{i=t+1}^n$. A weighted-graph-based test statistic is of the form

$$\max_t \left(\text{Strd} \left(w_0(t)d_{A(t)} + w_1(t)d_{B_1(t)} + w_2(t)d_{B_2(t)} \right) \right) \quad (3)$$

where different weights $w_0(t)$, $w_1(t)$, $w_2(t)$ lead to different statistics. Optimal weights depend on the distribution of data under H_A , and we propose new statistics motivated by $Z_w(t)$ and $Z_{\text{diff}}(t)$ and extend them to the multiple change points setting. Furthermore, in Section 3.3, we draw a connection between the proposed statistics and the existing nonparametric change point detection methods, allowing us to decompose the proposed statistics into a CUSUM form and to better understand their properties.

3.1 At Most One Change Point

We will introduce new statistics based on (3) where selection of $w_0(t)$, $w_1(t)$, $w_2(t)$ are motivated by Z_w and Z_{diff} .

Note that maximizing $Z_w(t)$ is equivalent to maximizing within-phase similarity, which is also equivalent to minimizing within-phase distance, i.e., $d_{B_1(t)}$ and $d_{B_2(t)}$. In addition, the between-phase distance, i.e., $d_{A(t)}$, should be maximized. This suggests choosing $w_0(t) >$

0, $w_1(t) < 0$, $w_2(t) < 0$ in (3). Under H_0 , we expect $\bar{d}_{A(t)} \approx \bar{d}_{B_1(t)} \approx \bar{d}_{B_2(t)}$, leading to the following statistic:

$$T_1(t) := \bar{d}_{A(t)} - \frac{1}{2}\bar{d}_{B_1(t)} - \frac{1}{2}\bar{d}_{B_2(t)}.$$

T_1 has mean zero under H_0 ; stabilizing the variance across t leads to the following test statistic

$$S_1 := \max_{n_0 \leq t \leq n_1} \frac{t(n-t)}{n} T_1(t), \quad (4)$$

where n_0, n_1 are pre-specified constraints for τ^* s.t. $n_0 = \lceil n\rho_0 \rceil, n_1 = \lceil n\rho_1 \rceil$ and $0 < \rho_0 < \rho^* < \rho_1 < 1$.

The intuition behind $Z_{\text{diff}}(t)$ is to maximize difference in within-phase similarities, which is equivalent to maximizing $d_{B_1(t)} - d_{B_2(t)}$. It suggests choosing $w_1(t) > 0, w_2(t) < 0, w_0(t) = 0$ in (3). Under H_0 , we expect that $\bar{d}_{B_1(t)} \approx \bar{d}_{B_2(t)}$ suggesting a test based on

$$T_2(t) = |\bar{d}_{B_1(t)} - \bar{d}_{B_2(t)}|.$$

Standardization leads to

$$S_2 := \max_{n_0 \leq t \leq n_1} \frac{1}{2\hat{s}_n} \sqrt{\frac{t(n-t)}{n}} T_2(t), \quad (5)$$

where the scaling factor $\hat{s}_n^2 = \frac{1}{n} \sum_{i=1}^n (\bar{d}_i)^2 - (\bar{d})^2$, $\bar{d}_i = \frac{1}{n} \sum_j d(y_i, y_j)$, $\bar{d} = \frac{1}{n^2} \sum_{i,j=1}^n d(y_i, y_j)$. Roughly speaking, \hat{s}_n^2 measures the variance in \bar{d}_i , and we refer the reader to the example below and Section 3.3 for more details.

S_1 and S_2 are scan statistics taking the maximum of a standardized score function across all possible change points. Rejection thresholds for S_1 and S_2 depend on the distance measure and the unknown null distribution of the data. The thresholds can be estimated using empirical samples as discussed in Section 4.1.1, where we also give analytic formulas for controlling type I error. When the test statistic is significant, the estimated change point $\hat{\tau}$ is defined as the time t where the maximum is taken.

The example below gives intuition on the mathematical decomposition underlying S_1 and S_2 .

An Illustrating Example Let $\{y_i\}_{i=1}^n$ be univariate normal, $F_0 = N(0, \sigma^2)$, and $d(y_i, y_j) = (y_i - y_j)^2$. Then,

$$T_1(t) = (\bar{y}_{t-} - \bar{y}_{t+})^2 + \mathcal{O}_p(n^{-1}), \quad (6)$$

where the first term corresponds to the z-statistic in likelihood ratio test for testing mean differences. It is also the CUSUM statistic for testing changes in $\mathbb{E}y_i$. Under the null,

$$nT_1(t) \xrightarrow{w} \sigma^2 [\rho(1 - \rho)]^{-1} (\chi_1^2 - 1),$$

when $t(n - t)/n^2 \rightarrow \rho(1 - \rho)$. Similarly,

$$T_2(t) = 2 |V(y, |\cdot|)_{t-} - V(y, |\cdot|)_{t+}| \quad (7)$$

measures the difference in estimated variance before and after t . It is the CUSUM of squares statistic for testing variance changes (Lee et al., 2003). Under the null,

$$n^{1/2} (\bar{d}_{B_1}(t) - \bar{d}_{B_2}(t)) \xrightarrow{w} 2\sigma^2 [\rho(1 - \rho)]^{-1/2} N(0, 2).$$

Thus, the scaling factor $\sqrt{t(n - t)/n} \approx \sqrt{n\rho(1 - \rho)}$ in Equation (5) cancels the effect of varying variances. And in this case we have $\hat{s}_n^2 = \frac{1}{n} \sum_{i=1}^n (y_i - \bar{y})^4 - [\frac{1}{n} \sum_{i=1}^n (y_i - \bar{y})^2]^2$. Thus \hat{s}_n converges in probability to $\sqrt{2}\sigma^2$.

In this example, Equation (6) and Equation (7) match the empirical conclusion from Chu et al. (2019) that Z_w (corresponding to T_1) is useful for detecting location changes while Z_{diff} (corresponding to T_2) is useful for detecting scale changes. In Section 3.3 we will see a similar CUSUM decomposition for *any* type of data and distance.

3.2 Multiple Change Points

In this section we show a bisection based procedure which generalizes the proposed statistics S_1 and S_2 to the multiple change point setting. Similar to the AMOC setting, we assume that $0 < \rho_0 \leq \frac{\rho_{k+1}^* - \rho_k^*}{\rho_{k+2}^* - \rho_k^*} \leq \rho_1 < 1$ for any $k = 1, 2, \dots, K - 2$. Based on this assumption, we define $S_1^{l,r}$, $T_1^{l,r}(t)$, $S_2^{l,r}$, $T_2^{l,r}(t)$, $\hat{s}_n^{l,r}$ as counterparts to $S_1, T_1, S_2, T_2, \hat{s}_n$ on the subsequence $\{y_l, \dots, y_r\}$: denote $l' = l + \lceil (r - l)\rho_0 \rceil$, $r' = l + \lceil (r - l)\rho_1 \rceil$, then

$$S_1^{l,r} := \max_{l' \leq t \leq r'} \frac{(t - l)(r - t)}{r - l} T_1^{l,r}(t), \quad \text{where} \quad T_1^{l,r}(t) := \bar{d}_{A^{l,r}(t)} - \frac{1}{2} \bar{d}_{B_1^{l,r}(t)} - \frac{1}{2} \bar{d}_{B_2^{l,r}(t)}, \quad (8)$$

and

$$S_2^{l,r} := \max_{l' \leq t \leq r'} \frac{1}{2\widehat{S}_n^{l,r}} \sqrt{\frac{(t-l)(r-t)}{r-l}} T_2^{l,r}(t), \quad (9)$$

where

$$T_2^{l,r}(t) := \left| \bar{d}_{B_1^{l,r}(t)} - \bar{d}_{B_2^{l,r}(t)} \right|,$$

$$[\widehat{S}_n^{l,r}]^2 = \frac{1}{r-l} \sum_{i=l}^r \left(\frac{1}{r-l} \sum_{j=l}^r d(y_i, y_j) \right)^2 - \left(\frac{1}{(r-l)^2} \sum_{i,j=l}^r d(y_i, y_j) \right)^2.$$

Then at each bisection iteration, for the current subsequence $\{y_l, \dots, y_r\}$, if we detect a change in distribution, we segment it at k where

$$k = \arg \max_{l' \leq t \leq r'} \frac{(t-l)(r-t)}{r-l} T_1^{l,r}(t) \quad \text{for } S_1, \text{ or} \quad (10)$$

$$k = \arg \max_{l' \leq t \leq r'} \frac{1}{2\widehat{S}_n^{l,r}} \sqrt{\frac{t(n-t)}{n}} T_2^{l,r}(t) \quad \text{for } S_2, \quad (11)$$

where $l' = l + \lceil \rho_0(r-l) \rceil$, $r' = l + \lceil \rho_1(r-l) \rceil$. The whole bisection procedure is summarized in Algorithm 1. Notice we do not allow segments with less than n_{\min} observations, which is set a priori in order to stabilize the performance.

3.3 Connections to Other Change Point Methods

We demonstrate here that our statistics are also related to various existing nonparametric CPD methods. Further, we will derive a similar CUSUM representation as in Equation (6) and (7) for any distance and any type of data.

First, the Euclidean-distance-based method (Matteson and James, 2014) is a special case of S_1 where d is the square distance. And Celisse et al. (2018); Sejdinovic et al. (2013) show that kernel-based and distance-based methods are essentially equivalent. In one direction, we can always define a kernel from a distance as long as it satisfies some mild conditions:

Lemma 3.1 (Lemma 12 in Sejdinovic et al. (2013)). *Define*

$$k^{(y_0)}(y_i, y_j) = \frac{1}{2} [d(y_i, y_0) + d(y_j, y_0) - d(y_i, y_j)] \quad (12)$$

Algorithm 1 Weighted-Graph-Based CPD for multiple change points

Input: Significance level α , minimum length n_{\min} .

Output: Set of detected change points $\hat{\mathcal{D}} = \text{BS}(1, n)$.

function BS(l, r)

Calculate the realization s of random variable $S := S_1^{l,r}$ or $S := S_2^{l,r}$.

Estimate the new change point k by Equation (10) or (11).

if $\mathbb{P}(S \geq s) \leq \alpha$ (using formulas in Section 4.1.1) and $k - l, r - k \geq n_{\min}$, **then**

Update $\hat{\mathcal{D}} \leftarrow \hat{\mathcal{D}} \cup \{k\}$.

Call BS(l, k).

Call BS($k + 1, r$).

end if

return $\hat{\mathcal{D}}$

end function

as the distance-induced kernel induced by $d(\cdot, \cdot)$ and centered at y_0 . Then $k^{(y_0)}$ is a valid kernel if and only if d is a semi-metric of negative type, i.e., if and only if d satisfies:

(1) $d(y_i, y_j) = 0$ if and only if $y_i = y_j$.

(2) $\forall y_i, y_j \in \mathcal{X}, d(y_i, y_j) = d(y_j, y_i)$.

(3) $\sum_{i,j=1}^n c_i c_j d(y_i, y_j) \leq 0, \forall n \geq 2, y_1, \dots, y_n \in \mathcal{X}, c_1, \dots, c_n \in \mathbb{R}, \sum_i c_i = 0$.

Remark 3.1. The notion of semi-metric of negative type encompasses a large collection of metric spaces, including L_p spaces for $0 < p \leq 2$. We refer the reader to Theorem 3.6 of Meckes (2013) for a list of examples of metrics spaces of negative type.

In the other direction, Proposition 14 in Sejdinovic et al. (2013) shows we can always define a distance from a kernel. Together with Lemma 3.1, it implies that kernel-based and distance-based methods are essentially equivalent.

Using Lemma 3.1, we find $T_1(t)$ equals the empirical maximum mean discrepancy Gretton et al. (2012) which was proposed for two sample testing. In this sense, S_1 shares similar intuition as Celisse et al. (2018); Sinn et al. (2012). Comparing with existing kernel methods, the proposed statistics are simple to compute, and have theoretical guarantees for both

detection and localization. For example, [Celisse et al. \(2018\)](#); [Sinn et al. \(2012\)](#) do not offer false positive controls. Statistic in [Harchaoui et al. \(2009\)](#) is more complicated to compute and do not provide guarantees on localization. [Li et al. \(2015\)](#) develop M-statistics which are computationally cheaper but require the availability of reference data.

Establishing the equivalence with kernel methods also allows us to use concepts in kernels to derive familiar CUSUM representations for a general d . For any y_0 , we define a centered kernel:

$$\tilde{k}(y_i, y_j) = k^{(y_0)}(y_i, y_j) - \mathbb{E}_{y_l \sim F_0} k^{(y_0)}(y_i, y_l) - \mathbb{E}_{y_l \sim F_0} k^{(y_0)}(y_l, y_j) + \mathbb{E}_{y_l, y_m \sim F_0} k^{(y_0)}(y_l, y_m). \quad (13)$$

It is easy to show \tilde{k} does not depend on y_0 (see Appendix Proposition 1). For \tilde{k} , we may write it in terms of eigenfunctions ψ_l with respect to the probability measure F_0 :

$$\begin{aligned} \tilde{k}(y, y') &= \sum_{l=1}^{\infty} \lambda_l \psi_l(y) \psi_l(y'), \quad \text{where} \\ \int \tilde{k}(y, y') \psi_l(y) dF_0(y) &= \lambda_l \psi_l(y'), \quad \int \psi_l(y) \psi_{l'}(y) dF_0(y) = \delta_{l,l'}. \end{aligned} \quad (14)$$

Denote the feature map ϕ as

$$\phi(y) = (\lambda_1^{1/2} \psi_1(y), \lambda_2^{1/2} \psi_2(y), \dots)^\top \in \mathcal{H}, \quad (15)$$

and $\langle \phi(y), \phi(y') \rangle_{\mathcal{H}} := \sum_{l=1}^{\infty} \phi_l(y) \phi_l(y') = \tilde{k}(y, y')$.

We investigate next the proposed statistics S_1, S_2 . Utilizing previous results, we have

$$T_1(t) = \|\bar{\phi}(y)_{t-} - \bar{\phi}(y)_{t+}\|_{\mathcal{H}}^2 + \mathcal{O}_p(n^{-1}), \quad (16)$$

where $\|\cdot\|_{\mathcal{H}} := \langle \cdot, \cdot \rangle_{\mathcal{H}}^{1/2}$ is the norm in \mathcal{H} . Intuitively $T_1(t)$ measures the difference between the average feature map between $\{y_i\}_{i=1}^t$ and $\{y_i\}_{i=t+1}^n$. For univariate data and Euclidean distance, this reduces to the example in Section 3.1. Notice that expression (16) has a familiar form as the CUSUM statistic ([Page, 1954](#)). Indeed, if we directly observe $\{\phi(y_i)\}_{i=1}^n$, S_1 equals the CUSUM statistic for Hilbert space valued data [Tewes \(2017\)](#). Similarly, we find

$$T_2(t) = 2 \left| V(\phi(y), \|\cdot\|_{\mathcal{H}})_{t-} - V(\phi(y), \|\cdot\|_{\mathcal{H}})_{t+} \right|, \quad (17)$$

Intuitively, if $\mathbb{E}\phi(y_i)$ does not change (here $\mathbb{E}\phi(y_i)$ is the mean feature map defined such that $\langle \mathbb{E}\phi(y), \phi(y_j) \rangle_{\mathcal{H}} = \mathbb{E}_y k(y, y_j)$), $T_2(t)$ measures the difference between the magnitude of noise $\epsilon_i = \phi(y_i) - \mathbb{E}\phi(y_i)$ in terms of $\|\cdot\|_{\mathcal{H}}$. Again, expression (17) exhibits the form of CUSUM statistics and can be seen as a generalization of the statistic in Lee et al. (2003), which is proposed for detecting changes in variance in time series models. Notice $\hat{s}_n^2 = 1/n \sum_{i=1}^n [\|\hat{\epsilon}_i\|_{\mathcal{H}}^2 - \sum_{i=1}^n \|\hat{\epsilon}_i\|_{\mathcal{H}}^2/n]^2$ is the empirical estimator for the variance of $\|\epsilon\|_{\mathcal{H}}^2$, where $\hat{\epsilon}_i = \phi(y_i) - \bar{\phi}(y)$ for $i = 1, \dots, n$.

The proposed method is also closely related to that of Dubey and Müller (2019) that developed a test statistic for detecting change point in Frechet mean and/or Frechet variance in the AMOC setting. Their statistics, before taking max with respect to t , is equivalent to (properly normalized) $4\tilde{T}_1^2(t) + T_2^2(t)$, where $\tilde{T}_1(t)$ is defined in Equation (26) and can be seen as a non-centered version of $T_1(t)$. In this sense S_1, S_2 and that of Dubey and Müller (2019) are highly related. One difference is that we analyze the two components, $T_1(t)$ and $T_2(t)$, separately, and the combination of them follows automatically (see Section 4.1.4). An advantage of using S_1 (or S_2) individually is that it achieves higher power and localization accuracy under local alternatives when a specific type of change occurs, as suggested by our theory and simulations. Moreover, by expressing S_1 and S_2 through $d_A(t), d_{B_1}(t), d_{B_2}(t)$, we are free of solving the optimization problem in Dubey and Müller (2019), granting the proposed statistics greater practicality. Finally, we also generalize our statistics to the multiple change points setting and prove next its asymptotic correctness.

4 Asymptotics

This section presents asymptotic guarantees for both AMOC and multiple change point setting. For $l = 0, 1, \dots, K$, we define $\mu_l = \mathbb{E}_{Y \sim F_l} \phi(Y)$ and $\sigma_l^2 = \mathbb{E}_{Y \sim F_l} \|\phi(Y) - \mu_l\|_{\mathcal{H}}^2$ with ϕ defined in (15). Throughout this section we assume:

$$d \text{ is a semi-metric of negative type.} \quad (\text{Assump 1})$$

Other than subsection 4.1.1, we also assume:

$$\exists M > 0, \forall i \in \{1, 2, \dots, n\}, \|\tilde{k}(y_i, y_i)\|^2 \leq M^2, \text{ a.s.} \quad (\text{Assump 2})$$

Proofs of results in this section are included in the Appendix.

4.1 At Most One Change Point

In AMOC setting, we provide guarantees for both detection (type I error, power) and localization (accuracy).

4.1.1 Approximations to Significance Levels

To control type I error, we focus on approximating tail distributions of S_1, S_2 under H_0 . We investigate utilizing their asymptotic null distribution, and also propose an improvement based on higher order corrections.

Asymptotic null distribution of S_1 and S_2 Notice that $\tilde{k}(y, y') = [\mathbb{E}_y d(y, y') + \mathbb{E}_{y'} d(y, y') - d(y, y') - \mathbb{E}_{y, y'} d(y, y')]/2$. Then we have:

Theorem 4.1 (Asymptotic null). *Under H_0 , as $n \rightarrow \infty$,*

(a) **For S_1 :** *there exists positive constant δ such that $\mathbb{E}_y |\tilde{k}(y, y)|^{2+\delta} + \mathbb{E}_{y, y'} |\tilde{k}(y, y')|^2 < +\infty$,*

$$S_1 \xrightarrow{w} \max_{\rho_0 \leq \rho \leq \rho_1} \frac{\sum_{l=1}^{\infty} \lambda_l (W_l^0(\rho)^2 - \rho(1 - \rho))}{\rho(1 - \rho)}, \quad (18)$$

where λ_l 's are defined in Equation (14).

(b) **For S_2 :** *there exists positive constant δ such that $\mathbb{E}_y |\tilde{k}(y, y) - \mathbb{E} \tilde{k}(y, y)|^{2+\delta} < +\infty$,*

$$S_2 \xrightarrow{w} \max_{\rho_0 \leq \rho \leq \rho_1} \left| \frac{1}{\sqrt{\rho(1 - \rho)}} W^0(\rho) \right|. \quad (19)$$

Remark 4.1. *In (a), the boundedness of $\mathbb{E}_y |\tilde{k}(y, y)|^{2+\delta}$ says $\mathbb{E} \|\phi(y)\|_{\mathcal{H}}^{4+2\delta}$ is finite so that the functional central limit theorem [Tewes \(2017\)](#) holds. And the boundedness of $\mathbb{E}_{y, y'} |\tilde{k}(y, y')|^2$ says $\int \tilde{k}(y, y')^2 dF_0(y) dF_0(y') < +\infty$, which ensures that eigen-decomposition (14) holds and*

SETTING	Z_w	M	S_1 (\tilde{S}_1 +CORRECTION)	S_2 (\tilde{S}_2 +CORRECTION)
$N(0, 1)$	0.06	0.1	0.07 (0.07)	0.06 (0.06)
$N(0, I_{10})$	0.05	0.06	0.06 (0.06)	0.02 (0.06)
$N(0, I_{50})$	0.12	0.13	0.06 (0.05)	0.15 (0.02)
$N(0, I_{100})$	0.08	0.15	0.09 (0.07)	0.45 (0.04)
$t(4)$	0.06	0.09	0.06 (0.06)	0.08 (0.08)
Pois(2)	0.15	1	0.09 (0.09)	0.04 (0.04)
χ_1^2	0.07	0.12	0.10 (0.11)	0.04 (0.05)

Table 1: Comparison of coverage probability under $\alpha = 0.05$. Set $n = 200$. Z_w, M (Chu et al., 2019) are using 1-MST and skewness correction in R package “gSeg” (Chen et al., 2015). All distances are set to Euclidean distance. Null distribution for S_1, \tilde{S}_1 uses empirical eigenvalues. Results are based on 200 simulations.

the right hand side of (18) is well-defined. In (b), finite $\mathbb{E}_y |\tilde{k}(y, y) - \mathbb{E}\tilde{k}(y, y)|^{2+\delta}$ implies finite $\mathbb{E} \|\phi(y)\|_{\mathcal{H}}^2 - \mathbb{E} \|\phi(y)\|_{\mathcal{H}}^2\|^{2+\delta}$, which guarantees that eigen-decomposition (14) and the weak convergence to Brownian motion (Doukhan, 2012) holds.

P-value approximation using asymptotic null distribution Type I error of the proposed tests can be controlled utilizing their asymptotic null distribution, where we can obtain approximate p-value via simulations. For S_1 , we can estimate the eigenvalues $\lambda_1, \lambda_2, \dots, \lambda_n$ by Equation (5) of Gretton et al. (2009), and then use simulations on the first $m \leq n$ sums to approximate the infinite sum.

P-value approximation using higher order corrections To investigate the accuracy of asymptotic approximations, we show coverage probability of S_1, S_2 under significance level $\alpha = 0.05$ (Table 1). For comparison, we also show estimates for Z_w, M (Chu et al., 2019). We observe that the approximation for S_1 works well, while S_2 becomes anti-conservative when dimensionality becomes high. Z_w and M are anti-conservative for Poisson and high dimensional normal. A closer look into S_2 reveals the reason: under H_0 ,

$$\frac{1}{\hat{s}_n} \sqrt{\frac{t(n-t)}{n}} T_2(t) = N(0, 1) + \mathcal{O}_p(n^{-1/2}),$$

where the last term depends on (i) magnitude of $\mathbb{E} \|\epsilon\|_{\mathcal{H}}^2$, and (ii) skewness of $\|\epsilon\|_{\mathcal{H}}^2$. Here $\epsilon = y - \phi(y)$. For $F_0 = N(0, I_p)$ where $I_p \in \mathbb{R}^{p \times p}$ is the identity matrix, as p becomes larger, $\mathbb{E} \|\epsilon\|^2$ increases and thus, the $\mathcal{O}_p(n^{-1/2})$ term becomes increasingly in-negligible. To reduce the bias from $\mathbb{E} \|\epsilon\|^2$, we suggest using \tilde{S}_2 instead of S_2 , where

$$\tilde{S}_2 = \max_{n_0 \leq t \leq n_1} \frac{1}{2\hat{s}_n} \sqrt{\frac{t(n-t)}{n}} \tilde{T}_2(t), \quad (20)$$

with \tilde{T}_2 defined as

$$\tilde{T}_2(t) = \left| \bar{d}_{B_1(t)} - \bar{d}_{B_2(t)} - \frac{2\widehat{\mathbb{E}\|\epsilon\|^2}}{\sqrt{n\rho(1-\rho)}} \left(\frac{2t}{n} - 1 \right) \right|, \quad \text{where } \widehat{\mathbb{E}\|\epsilon\|^2} = \frac{1}{2n^2} \sum_{i \neq j, i, j=1}^n d(y_i, y_j). \quad (21)$$

To further alleviate the bias from the skewness of $\|\epsilon\|_{\mathcal{H}}^2$, following [Chen et al. \(2015\)](#), we propose a skewness correction:

$$\mathbb{P}(\tilde{S}_2 \geq x) \approx x\varphi(x) \int_{\rho_0}^{\rho_1} \left[1 + \frac{Vx(x^2 - 3)}{6\sqrt{n}} \right] \frac{1}{u(1-u)} \nu \left(\sqrt{\frac{x}{u(1-u)n}} \right) du, \quad (22)$$

where φ is the density function of standard normal, $\nu(\cdot)$ is defined as

$$\nu(x) = \frac{(2/x)(\Phi(x/2) - 0.5)}{(x/2)\Phi(x/2) + \varphi(x/2)}, \quad (23)$$

where Φ are the cumulative distribution function for standard normal. And V is defined as

$$V = \frac{1 - 2u}{\sqrt{u(1-u)}} \frac{m_6 - 3m_2m_4 + 2m_2^3}{\hat{s}_n^3}, \quad (24)$$

where m_i is the sample i -th moment of $\|\phi(y)\|_{\mathcal{H}}$ under the null. The expressions for m_2, m_4, m_6 are

$$\begin{aligned} m_2 &= \frac{1}{2n^2} \sum_{i \neq j} d(y_i, y_j), \\ m_4 &= \frac{1}{4n} \sum_{i=1}^n \left[\frac{2}{n} \sum_{j=1}^n d(y_i, y_j) - \frac{1}{n^2} \sum_{l, j=1}^n d(y_l, y_j) \right]^2, \\ m_6 &= \frac{1}{8n} \sum_{i=1}^n \left[\frac{2}{n} \sum_{j=1}^n d(y_i, y_j) - \frac{1}{n^2} \sum_{l, j=1}^n d(y_l, y_j) \right]^3. \end{aligned} \quad (25)$$

Coverage probabilities using \tilde{S}_2 and (22) are shown in brackets in Table 1. The gain of using higher order correction becomes significant as $\mathbb{E}\|\epsilon\|^2$ or the skewness of $\|\epsilon\|^2$ becomes larger, and it is not only in terms of p-value calibration, but also in terms of localization. So we suggest using \tilde{S}_2 instead of S_2 , especially when data dimension is high. Notice that theoretical properties of S_2 hold also for \tilde{S}_2 (Theorem 4.1, 4.2, 4.3).

For S_1 , notice that under H_0 ,

$$\frac{t(n-t)}{n}T_1(t) = \sum \lambda_l(\chi_1^2 - 1) + \mathcal{O}_p(n^{-1/2}),$$

where last term depends on (i) $\mathbb{E}d(y_i, y_j)$ and (ii) the skewness of each dimension of $\phi(y_i)$. Correcting for (ii) is complicated; and the terms resulting in (i) come from d_{B_1}, d_{B_2} . We can change the weight before d_{B_1}, d_{B_2} to eliminate (i):

$$\tilde{S}_1 = \max_{n_0 \leq t \leq n_1} \frac{t(n-t)}{n} \tilde{T}_1(t), \quad (26)$$

where $\tilde{T}_1(t) = \frac{d_{A(t)}}{t(n-t)} - \frac{d_{B_1(t)}}{2t^2} - \frac{d_{B_2(t)}}{2(n-t)^2}$. Recall $T_1(t) = \frac{d_{A(t)}}{t(n-t)} - \frac{d_{B_1(t)}}{2t(t-1)} - \frac{d_{B_2(t)}}{2(n-t)(n-t-1)}$. Notice

$$\tilde{T}_1(t) = \|\bar{\phi}(y)_{t-} - \bar{\phi}(y)_{t+}\|_{\mathcal{H}}^2 \geq 0.$$

Power and localization consistency (Theorem 4.3, 4.2) also hold for \tilde{S}_1 , while its asymptotic null distribution becomes

$$\tilde{S}_1 \xrightarrow{w} \max_{\rho_0 \leq \rho \leq \rho_1} \frac{\sum_{l=1}^{\infty} \lambda_l W_l^0(\rho)^2}{\rho(1-\rho)},$$

where the right hand side is well-defined if $\sum_l \lambda_l < \infty$ or simply, when d is bounded. Coverage probabilities using \tilde{S}_1 are shown in brackets in Table 1. As the original S_1 already performs quite well, the gain of using \tilde{S}_1 is not significant.

4.1.2 Power

The following theorems demonstrate the power consistency of proposed tests under contiguous alternatives.

Theorem 4.2 (Power Consistency). *We have*

(a) **For S_1** : If $\sqrt{n}\|\mu_0 - \mu_1\|_{\mathcal{H}} \rightarrow \infty$, then

$$\mathbb{P}_{H_A}(S_1 > q_\alpha^{(1)}) \rightarrow 1, \quad n \rightarrow \infty$$

with $q_\alpha^{(1)}$ the upper α -th quantile of asymptotic null of S_1 .

(b) **For S_2** : If $\mu_0 = \mu_1$ and $\sqrt{n}|v_0 - v_1| \rightarrow \infty$, then

$$\mathbb{P}_{H_A}(S_2 > q_\alpha^{(2)}) \rightarrow 1, \quad n \rightarrow \infty$$

with $q_\alpha^{(2)}$ the upper α -th quantile of asymptotic null of S_2 .

Remark 4.2. We show the power consistency of S_1 and S_2 even when the difference between F_0 and F_1 measured in terms of $\|\mu_0 - \mu_1\|_{\mathcal{H}}$ or $|v_0 - v_1|$ shrinks to zero at a rate slower than $n^{-1/2}$. Conclusion (2) shows that S_2 is a complement to S_1 in the sense that it is useful when change in distributions cannot be captured by $\mathbb{E}\phi(y)$.

Theorem 4.2 guarantees that with more data, we will eventually detect the change point as long as it is captured by μ or v . We will see next that localization accuracy also depends on μ, v . Here μ, v are determined by d and thus, the choice of d is critical for the performance of proposed statistics. However, the choice of proper distance is not the main focus of this article, and thus we simply assume that it is given.

4.1.3 Minimax Localization Rate

This section is concerned with the consistency of localization after detection of a change point.

Theorem 4.3 (Localization consistency). *We have*

(a) **For S_1** : If μ_0, μ_1 are fixed and $\mu_0 \neq \mu_1$, then for any $x > 0$ and n , with probability at least $1 - 22e^{-x}$, we have

$$\left| \frac{\hat{\tau} - \tau^*}{n} \right| \leq \frac{C_1}{n} \left(\frac{M^2 x}{\|\mu_0 - \mu_1\|_{\mathcal{H}}^2} + \frac{M^4 x}{\|\mu_0 - \mu_1\|_{\mathcal{H}}^4} \right),$$

where $\hat{\tau}$ is the estimated change point using statistics S_1 and C_1 is some constant depending on ρ_0, ρ_1, ρ^* .

(b) **For S_2** : If $\mu_0 = \mu_1$, v_0, v_1 are fixed and $v_0 \neq v_1$, then for any $x > 0$, when sample size n is sufficiently large, with probability at least $1 - 16e^{-x}$, we have

$$\left| \frac{\hat{\tau} - \tau^*}{n} \right| \leq \frac{C_2}{n} \left(\frac{M^4 x}{|v_0 - v_1|^2} + \frac{M^2 x}{|v_0 - v_1|} \right),$$

where $\hat{\tau}$ is the estimated change point using statistics S_2 and C_2 is some constant depending on ρ_0, ρ_1, ρ^* .

Theorem 4.3 shows that under suitable d , the location of estimated change point is rate optimal (Brunel, 2014).

4.1.4 Combining S_1, S_2 for Unknown Type of Change

To increase power, we could combine S_1, S_2 to detect unknown type of changes. However, differently from (unweighted) graph-based CPD methods where Z_w, Z_{diff} are always independent (Chu et al., 2019), S_1, S_2 are independent only under some restrictive conditions (Proposition 2 in the Appendix). Thus, combining S_1, S_2 in general case is much more complicated. Notice that the order of $T_1(t)$ and $T_2(t)$ are different. The work from Dubey and Müller (2019) motivates one simple way to combine S_1 and S_2 :

$$S_3 = \max_{n_0 \leq t \leq n_1} \frac{1}{4\widehat{\mathcal{S}}_n^2} \frac{t(n-t)}{n} [4T_1^2(t) + T_2^2(t)]. \quad (27)$$

As corollaries of previous theorems, we can get asymptotic null distribution, power, and localization consistency of S_3 . The results are similar to those in Dubey and Müller (2019) and for brevity are included in the Appendix B.8. Comparing Corollary B.3 or Theorem 3 in Dubey and Müller (2019) against Theorem 4.2, we find that when using S_3 instead of S_1 , we are capable of identifying both changes in location or scale, but pay a price of increasing the order of magnitude of local alternatives $\|\mu_0 - \mu_1\|_{\mathcal{H}}$ we can detect from $n^{-1/2}$ to $n^{-1/4}$.

4.2 Multiple Change Points

Theoretical guarantees of the proposed method in multiple change points setting are provided. We show that asymptotically, under some mild conditions, we can identify both the

correct number and locations of change points:

Theorem 4.4. *In multiple change points setting, we have*

(a) **For \mathbf{S}_1 :** *If $\exists c_1 > 0$ s.t. $\|\mu_l - \mu_{l+1}\|_{\mathcal{H}} \geq c_1$ for any $l = 0, 1, \dots, K - 1$, Algorithm 1 for S_1 yields: as $n \rightarrow \infty, \alpha \rightarrow 0, n\alpha \rightarrow \infty$,*

$$\mathbb{P}\left(|\hat{\mathcal{D}}| = |\mathcal{D}|\right) \rightarrow 1, \quad \text{and} \quad \forall k \in \hat{\mathcal{D}}, \quad \min_{\tau \in \mathcal{D}} |k/n - \tau/n| = o_p(1). \quad (28)$$

(b) **For \mathbf{S}_2 :** *If $\mu_0 = \mu_1 = \dots = \mu_K$ and there exists some constant c_2 s.t. $|\sigma_l^2 - \sigma_{l+1}^2| \geq c_2 > 0$ for any $l = 0, 1, \dots, K - 1$, Algorithm 1 for S_2 also yields (28) as $n \rightarrow \infty, \alpha \rightarrow 0, \sqrt{n}\alpha \rightarrow \infty$.*

5 Power and Localization Comparison

We investigate the power and localization accuracy for the proposed statistics in simulated datasets. We compare the proposed statistics (S_1, S_2, S_3 , all with higher order corrections introduced in Section 4.1.1) against Z_w, M and that of [Dubey and Müller \(2019\)](#), which we refer to as D . Notice that S_3 is the same as D (see Definition 27), except that we are using higher order corrections introduced in Section 4.1.1. For graph-based methods, as suggested by [Chen and Friedman \(2017\)](#), we use 5-MST to construct the graph. We investigate high-dimensional data (normal distributed unless specifically noted), Erdos-Renyi random graph, and functional data. Denote $\mathbf{1}_d \in \mathbb{R}^d$ as the vector of all 1's, $I_d \in \mathbb{R}^{d \times d}$ as the identity matrix.

5.1 AMOC Setting

We set $n = 100, \tau^* = 33$ and report: (1) the empirical probability of correctly detecting the change point and (2) the L_1 error in locating the change point, both averaged over 100 simulations. For fairness, we use 1000 permutations to compute the p-values for all methods. Results are summarized in Table 2.

For Euclidean data, we set $d(y, y') = \|y - y'\|^2$ where $\|\cdot\|$ is Euclidean distance. We compare (multivariate) Gaussian and Poisson distribution. When only mean changes, we

DIM	μ_1	σ_1	Z_w	M	S_1	S_2	S_3	D
1	0.8	-	0.41 (15.12)	0.40 (17.68)	0.85 (6.01)	0.05 (29.78)	0.23 (18.77)	0.27 (16.52)
10	0.3	-	0.41 (19.98)	0.35 (21.77)	0.66 (8.43)	0.03 (28.09)	0.04 (26.73)	0.06 (31.46)
50	0.2	-	0.33 (14.13)	0.27 (18.07)	0.90 (4.11)	0.01 (33.00)	0.02 (28.64)	0.05 (39.92)
100	0.2	-	0.57 (11.59)	0.46 (13.64)	0.98 (2.40)	0.05 (34.21)	0.07 (24.88)	0.07 (41.45)
500	0.1	-	0.33 (17.24)	0.26 (18.69)	0.75 (7.21)	0.02 (38.07)	0.02 (38.67)	0.06 (45.29)
1	-	2	0.39 (15.71)	0.39 (18.78)	0.07 (37.36)	0.49 (13.46)	0.44 (13.49)	0.59 (12.09)
10	-	1.2	0.13 (19.98)	0.45 (11.64)	0.02 (32.53)	0.77 (8.27)	0.77 (8.28)	0.80 (7.89)
50	-	1.06	0.06 (25.73)	0.33 (13.56)	0.05 (33.71)	0.54 (13.34)	0.52 (14.49)	0.44 (17.20)
100	-	1.05	0.04 (25.16)	0.24 (13.94)	0.03 (32.88)	0.64 (11.20)	0.63 (11.25)	0.23 (16.95)
500	-	1.03	0.12 (23.50)	0.70 (8.89)	0.09 (30.67)	0.82 (5.79)	0.81 (6.28)	0.24 (30.64)
1	2	2	0.53 (10.81)	0.53 (12.82)	0.39 (16.51)	0.47 (9.30)	0.52 (9.18)	0.65 (7.65)
10	0.6	1.2	0.45 (10.24)	0.55 (7.98)	0.44 (9.05)	0.81 (6.53)	0.83 (5.77)	0.90 (5.75)
50	0.4	1.06	0.41 (11.61)	0.43 (12.32)	0.80 (8.09)	0.49 (9.62)	0.51 (7.93)	0.36 (18.88)
100	0.4	1.05	0.00 (42.15)	0.00 (42.15)	1.00 (2.65)	0.62 (9.03)	0.71 (6.54)	0.25 (19.48)
500	0.2	1.03	0.47 (9.06)	0.60 (9.96)	0.74 (4.93)	0.74 (5.08)	0.74 (4.96)	0.19 (30.47)
1 (POISSON)	$\times 2$	$\times \sqrt{2}$	1.00 (11.41)	1.00 (11.36)	0.99 (3.69)	0.02 (20.16)	0.60 (6.64)	0.69 (5.98)

(a) Euclidean, high-dimensional data.

F_1	Z_w	M	S_1	S_2	S_3	D
$p_1 = 0.3$	0.62 (12.93)	0.49 (12.19)	0.98 (4.18)	0.30 (17.45)	0.33 (15.61)	0.29 (18.47)
$p_1 = 0.4$	1.00 (2.62)	0.97 (2.66)	1.00 (0.92)	0.62 (8.03)	0.80 (4.72)	0.63 (11.55)
$p_1 = 0.5$	1.00 (1.01)	1.00 (1.01)	1.00 (0.31)	0.67 (9.43)	0.96 (2.89)	0.85 (5.44)

(b) Network data.

F_1	Z_w	M	S_1	S_2	S_3	D
$\mu = 0.03$	0.08 (30.02)	0.09 (28.22)	0.09 (25.81)	0.05 (41.94)	0.05 (41.60)	0.08 (48.06)
$\mu = 0.05$	0.12 (24.19)	0.11 (25.51)	0.44 (14.97)	0.04 (46.70)	0.03 (47.04)	0.05 (43.30)
$\mu = 0.08$	0.68 (9.02)	0.56 (11.05)	1.00 (1.46)	0.02 (49.76)	0.03 (49.08)	0.03 (40.24)
$\mu = 0.10$	0.99 (4.00)	0.95 (4.50)	1.00 (0.46)	0.02 (44.32)	0.02 (44.32)	0.07 (45.68)

(c) Function data.

Table 2: Comparison of power and localization accuracy for each method in AMOC setting. We report the proportion of experiments with p-value smaller than 0.05, out of 100 replications. Number in brackets are the localization error $|\hat{\tau} - \tau^*|$ averaged over 100 replications.

set $F_0 = N(0 \times \mathbf{1}_d, I_d)$, $F_1 = \mu_1 \times \mathbf{1}_d + F_0$. We observe that S_1 consistently outperforms other methods by a large margin, both in terms of power and localization accuracy. S_3 and D , although combining information from S_1 , have inferior performance because they put larger weights (of higher order) on S_2 . When only scale changes, we set $F_0 = N(0 \times \mathbf{1}_d, I_d)$, $F_1 = \sigma_1 F_0$. We see that in low to moderate dimensions, S_2, S_3 and D have the best performance; in high dimensions, higher order corrections become important and thus, S_2 and S_3 become superior than D . When both mean and scale change, we set $F_0 = N(0 \times \mathbf{1}_d, I_d)$, $F_1 = \mu_1 \times \mathbf{1}_d + \sigma_1 F_0$ on normal data and $F_0 = \text{Poisson}(2)$, $F_1 = \text{Poisson}(4)$ on Poisson data. We see that in low dimensions, S_1, S_2, D are performing well, and D is slightly better than S_1, S_2 . However when dimensionality grows high, D becomes inferior and depending on the actual magnitude of changes, it is often one of S_1, S_2, S_3 that performs the best.

For network data, we use Erdos-Renyi random graph with 10 nodes. Before change point, an edge is formed independently between two nodes with probability $p_0 = 0.1$. After change point, a community emerges among the first 3 nodes, the probability of forming an edge within which becomes p_1 . The probability of forming an edge among other pairs remains 0.1. We use $d(y, y') = \|y - y'\|_F^2$ where $\|\cdot\|_F$ is the Frobenius norm and y is the adjacency matrix where an edge is represented by 1 and otherwise 0. As suggested by Table 2, S_1 outperforms all other methods.

For functional data, suppose each y_i is a noisy observation of a discretized function at 1000 equally spaced grids. Set $y_i(x) = \sin(x) + 0.5N(0, 1)$, $x \in [0, 2\pi]$ for $i = 1, 2, \dots, \tau^*$ and $y_i(x) = \sin(x + \mu) + 0.5N(0, 1)$, $x \in [0, 2\pi]$ for $i = \tau^* + 1, \dots, n$. We use distance $d(y, y') = \int_0^{2\pi} |y(x) - y'(x)|^2 dx$. Table 2 reveals that S_1 consistently has the best performance.

5.2 Multiple Change Points Setting

We set $n = 150$, $\tau_1^* = 40$, $\tau_2^* = 100$. Following [Matteson and James \(2014\)](#), we use Rand Index defined below to measure the performance of each method.

Definition 5.1 (Rand Index). *For any two clusterings U, V of n observations, the Rand*

DIM	μ_1	μ_2	Z_w	M	S_1	S_2	S_3	D
1	2	1	0.87	0.72	0.92	0.55	0.78	0.78
10	0.5	0.2	0.67	0.57	0.73	0.34	0.34	0.37
50	0.5	0.2	0.67	0.57	0.73	0.34	0.54	0.37
100	0.3	0.1	0.61	0.56	0.99	0.34	0.45	0.38
500	0.2	0.1	0.57	0.57	0.88	0.34	0.34	0.34

DIM	σ_1	σ_2	Z_w	M	S_1	S_2	S_3	D
1	2	$\sqrt{2}$	0.81	0.71	0.41	0.92	0.92	0.92
10	1.2	1.2	0.48	0.63	0.41	0.95	0.95	0.97
50	1.06	1.06	0.34	0.63	0.34	0.83	0.78	0.76
100	1.05	1.05	0.49	0.55	0.34	0.92	0.92	0.71
500	1.03	1.03	0.38	0.67	0.34	0.89	0.89	0.69

(a) High-dimensional data, mean change.

(b) High-dimensional data, scale change.

DIM	μ_1	σ_1	μ_2	σ_2	Z_w	M	S_1	S_2	S_3	D
1	2	2	1	$\sqrt{2}$	0.82	0.72	0.67	0.47	0.47	0.72
10	0.6	1.2	0.3	1.2	0.56	0.61	0.82	0.95	0.95	0.95
50	0.4	1.06	0.2	1.06	0.93	0.71	0.996	0.78	0.86	0.81
100	0.4	1.05	0.2	1.05	0.55	0.50	0.92	0.95	0.95	0.69
500	0.2	1.03	0.1	1.03	0.72	0.72	0.92	0.95	0.95	0.73
1 (POISSON)	$\times 1.5$	$\times \sqrt{1.5}$	$\times 1$	$\times 1$	0.51	0.51	0.91	0.41	0.73	0.76

(c) High-dimensional data, both mean and scale change.

F_1	Z_w	M	S_1	S_2	S_3	D
$p_1 = 0.3$	0.40	0.40	0.70	0.52	0.52	0.52
$p_1 = 0.4$	0.59	0.48	0.91	0.53	0.53	0.49
$p_1 = 0.5$	0.83	0.66	0.93	0.74	0.87	0.75

F_1	Z_w	M	S_1	S_2	S_3	D
$\mu = 0.03$	0.34	0.34	0.41	0.34	0.34	0.34
$\mu = 0.05$	0.34	0.34	0.47	0.34	0.34	0.34
$\mu = 0.08$	0.34	0.34	0.81	0.34	0.34	0.34
$\mu = 0.1$	0.55	0.55	0.83	0.34	0.34	0.34

(d) Network data.

(e) Functional data

Table 3: Comparison of Rand Index (Rand, 1971) (averaged over 100 replications) computed by R package “fossil” (Vavrek, 2015) for different methods in multiple change points setting. We set $n = 150$, $\tau_1^* = 40$, $\tau_2^* = 100$.

Index is defined as

$$Rand = \frac{\#I_1 + \#I_2}{\binom{2}{n}}$$

where $\#I_1$ is the number of pairs in the same cluster under U and V , and $\#I_2$ is the number of pairs in different clusters under U and V .

Rand Index incorporates information from both power and localization accuracy, and higher value means better performance. In practice we compute Rand Index by R package “fossil” (Vavrek, 2015). Originally Z_w, M and D are not designed for multiple change points setting, but we generalize them using a similar binary segmentation procedure as in Algorithm 1 (we use $n_{\min} = 20, \alpha = 0.05$). Results are shown in Table 3.

For Euclidean data, when there is only mean change, we set $F_0 = N(0 \times \mathbf{1}_d, I_d)$, $F_1 = \mu_1 \times \mathbf{1}_d + F_0$, $F_2 = \mu_2 \times \mathbf{1}_d + F_0$. Table 3a shows that S_1 has the best performance. When there is only scale change, we set $F_0 = N(0 \times \mathbf{1}_d, I_d)$, $F_1 = \sigma_1 F_0$, $F_2 = \sigma_2 F_0$. Observe that S_2 has the best performance. When there are changes in both mean and scale, we set $F_0 = N(0 \times \mathbf{1}_d, I_d)$, $F_1 = \mu_1 \times \mathbf{1}_d + \sigma_1 F_0$, $F_2 = \mu_2 \times \mathbf{1}_d + \sigma_2 F_0$ on normal data and $F_0 = F_2 = \text{Poisson}(4)$, $F_1 = \text{Poisson}(6)$ on Poisson data. Depending on the actual magnitude of changes, one of S_1, S_2, S_3 has the best performance. And the gain of using S_3 instead of D becomes larger as dimensionality becomes larger.

For network data, we use Erdos-Renyi random graph with 10 nodes. For F_0 and F_2 , an edge is formed independently between two nodes with probability $p_0 = 0.1$. For F_1 , a community emerges among the first 3 nodes, the probability of forming an edge within which becomes p_1 . The probability of forming an edges among other pairs remains $p_0 = 0.1$. We observe in Table 3d that S_1 has the best performance.

For functional data, for F_0 , we set $y_i(x) = \sin(x) + 0.5N(0, 1), x \in [0, 2\pi]$; for F_1 , $y_i(x) = \sin(x+2\mu)+0.5N(0, 1), x \in [0, 2\pi]$; for F_2 , $y_i(x) = \sin(x+\mu)+0.5N(0, 1), x \in [0, 2\pi]$. The other settings are identical to the AMOC setting. We observe in Table 3e that S_1 has the best performance.

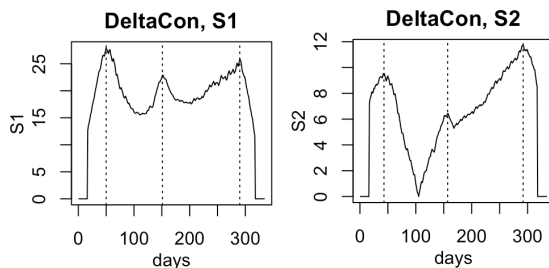


Figure 1: Plot of S_1, S_2 on MIT proximity network data. The peaks correspond to the change points detected by Algorithm 1.

Conclusion In both AMOC and multiple change points setting, the proposed statistics outperform baselines. If we know the type of change, using the corresponding S_1 (or S_2) is highly advantageous. Higher order corrections are useful, especially under high dimensions where it greatly improves both power and localization accuracy. For unknown type of change, which one of S_1, S_2, S_3 performs best is dependent on the actual distribution. We can either apply S_3 , considering its relative robust performance across different types of changes; or we can apply S_1 and S_2 separately.

6 Real Data Analysis

The MIT proximity network is extracted from the MIT Reality Mining dataset (Pentland et al., 2009), which consists of the proximity network for $m = 93$ faculty and graduate students recorded via cell phone Bluetooth scan every five minutes. From the raw data, we extracted a sequence of daily binary networks $\{y_i\}_{i=1}^n \in \mathbb{R}^{m \times m}$ from July 2004 to June 2005, where a link between two subjects means that they are scanned together at least once during that day. We used DELTACON (Koutra et al., 2013) to measure the distance $d(y_i, y_j)$, which is defined as

$$d(y_i, y_j) = \left[\sum_{k=1}^m \sum_{l=1}^m (\sqrt{q_{i,kl}} - \sqrt{q_{j,kl}})^2 \right]^{1/2},$$

where $Q_i := [q_{i,kl}]_{k,l=1}^m = (I_m + \epsilon_i^2 U_i - \epsilon_i y_i)^{-1} \in \mathbb{R}^{m \times m}$, $\epsilon_i = \frac{1}{1 + \max_k(c_{k,k}^i)}$ with $c_{k,k}^i$ the degree of the k -th subject in the i -th network, and $U_i = \text{diag}(c_{1,1}^i, \dots, c_{m,m}^i)$.

The scan statistic on the original sequence is shown in Figure 1. Using Algorithm 1, we identify the 50th (2004/9/6), 151st (2004/12/17), and 290th (2005/5/4) day as change points. They correspond to the first day of class (2004/9/8), end of exam week (2004/12/17), and the last day of classes (2005/5/12), all with p-value approximately equal to 0. Using S_2 identifies very similar change points. Different distance measures (Frobenius, NetSimile (Berlengerio et al., 2012)) led to similar results.

7 Discussion and Conclusion

We propose nonparametric scan statistics for the detection and localization of change points based on the graph-based CPD framework. The proposed statistics are applicable to both AMOC and multiple change points setting. We provide analytic forms to control type I error of the proposed statistics, as well as prove their power consistency and minimax localization rate. This work also establishes connections among various CPD methods. In particular, we found that the graph-based statistics Z_w, Z_{diff} (Chu et al., 2019) exhibit similar forms as the familiar CUSUM statistic, which justifies the empirical observations on their performance.

The performance of the statistics is determined by both the magnitude of change and the distance measure. Ideally the distance d should be able to capture all possible changes in the distribution. In the extreme case where the change in distribution is not reflected by d (more precisely, the feature map ϕ associated with d), the proposed statistics will lack power. Thus, distance selection or distance learning from data is an important topic which needs further investigation.

References

Arlot, S., A. Celisse, and Z. Harchaoui (2012). A kernel multiple change-point algorithm via model selection. *arXiv:1202.3878*.

- Arlot, S., A. Celisse, and Z. Harchaoui (2019). A kernel multiple change-point algorithm via model selection. *Journal of machine learning research* 20(162).
- Berlinet, A. and C. Thomas-Agnan (2011). *Reproducing kernel Hilbert spaces in probability and statistics*. Springer Science & Business Media.
- Berlingerio, M., D. Koutra, T. Eliassi-Rad, and C. Faloutsos (2012). Netsimile: A scalable approach to size-independent network similarity. *arXiv:1209.2684*.
- Brunel, V.-E. (2014). Convex set detection. *arXiv:1404.6224*.
- Celisse, A., G. Marot, M. Pierre-Jean, and G. Rigail (2018). New efficient algorithms for multiple change-point detection with reproducing kernels. *Computational Statistics & Data Analysis* 128, 200–220.
- Chang, W.-C., C.-L. Li, Y. Yang, and B. Póczos (2019). Kernel change-point detection with auxiliary deep generative models. *arXiv:1901.06077*.
- Chen, H. (2019). Change-point detection for multivariate and non-euclidean data with local dependency. *arXiv:1903.01598*.
- Chen, H. et al. (2019). Sequential change-point detection based on nearest neighbors. *The Annals of Statistics* 47(3), 1381–1407.
- Chen, H., X. Chen, and Y. Su (2018). A weighted edge-count two-sample test for multivariate and object data. *Journal of the American Statistical Association* 113(523), 1146–1155.
- Chen, H. and J. H. Friedman (2017). A new graph-based two-sample test for multivariate and object data. *Journal of the American statistical association* 112(517), 397–409.
- Chen, H., N. Zhang, et al. (2015). Graph-based change-point detection. *The Annals of Statistics* 43(1), 139–176.

- Chen, H., N. Zhang, and L. Chu (2015). gseg: Graph-based change-point detection (g-segmentation). r package, version 0.1.
- Chu, L. and H. Chen (2018). Sequential change-point detection for high-dimensional and non-euclidean data. *arXiv:1810.05973*.
- Chu, L., H. Chen, et al. (2019). Asymptotic distribution-free change-point detection for multivariate and non-euclidean data. *The Annals of Statistics* 47(1), 382–414.
- Desobry, F., M. Davy, and C. Doncarli (2005). An online kernel change detection algorithm. *IEEE Transactions on Signal Processing* 53(8), 2961–2974.
- Doukhan, P. (2012). *Mixing: properties and examples*, Volume 85. Springer Science & Business Media.
- Dubey, P. and H.-G. Müller (2019). Frechet change point detection. *arXiv:1911.11864*.
- Friedman, J. H. and L. C. Rafsky (1979). Multivariate generalizations of the wald-wolfowitz and smirnov two-sample tests. *The Annals of Statistics*, 697–717.
- Garreau, D., S. Arlot, et al. (2018). Consistent change-point detection with kernels. *Electronic Journal of Statistics* 12(2), 4440–4486.
- Gretton, A., K. M. Borgwardt, M. J. Rasch, B. Schölkopf, and A. Smola (2012). A kernel two-sample test. *Journal of Machine Learning Research* 13(Mar), 723–773.
- Gretton, A., K. Fukumizu, Z. Harchaoui, and B. K. Sriperumbudur (2009). A fast, consistent kernel two-sample test. In *Advances in neural information processing systems*, pp. 673–681.
- Harchaoui, Z., E. Moulines, and F. R. Bach (2009). Kernel change-point analysis. In *Advances in neural information processing systems*, pp. 609–616.

- Harchaoui, Z., F. Vallet, A. Lung-Yut-Fong, and O. Cappé (2009). A regularized kernel-based approach to unsupervised audio segmentation. In *2009 IEEE International Conference on Acoustics, Speech and Signal Processing*, pp. 1665–1668. IEEE.
- Henze, N. (1988). A multivariate two-sample test based on the number of nearest neighbor type coincidences. *The Annals of Statistics*, 772–783.
- Huang, S., Z. Kong, and W. Huang (2014). High-dimensional process monitoring and change point detection using embedding distributions in reproducing kernel hilbert space. *IIE Transactions* 46(10), 999–1016.
- Koutra, D., J. T. Vogelstein, and C. Faloutsos (2013). Deltacon: A principled massive-graph similarity function. In *Proceedings of the 2013 SIAM International Conference on Data Mining*, pp. 162–170. SIAM.
- Lee, S., O. Na, and S. Na (2003). On the cusum of squares test for variance change in nonstationary and nonparametric time series models. *Annals of the Institute of Statistical Mathematics* 55(3), 467–485.
- Li, S., Y. Xie, H. Dai, and L. Song (2015). M-statistic for kernel change-point detection. In *Advances in Neural Information Processing Systems*, pp. 3366–3374.
- Li, Z., P. Li, A. Krishnan, and J. Liu (2011). Large-scale dynamic gene regulatory network inference combining differential equation models with local dynamic bayesian network analysis. *Bioinformatics* 27(19), 2686–2691.
- Liu, Y.-W. and H. Chen (2020). A fast and efficient change-point detection framework for modern data. *arXiv:2006.13450*.
- Lu, T., H. Liang, H. Li, and H. Wu (2011). High-dimensional odes coupled with mixed-effects modeling techniques for dynamic gene regulatory network identification. *Journal of the American Statistical Association* 106(496), 1242–1258.

- Matteson, D. S. and N. A. James (2014). A nonparametric approach for multiple change point analysis of multivariate data. *Journal of the American Statistical Association* 109(505), 334–345.
- Meckes, M. W. (2013). Positive definite metric spaces. *Positivity* 17(3), 733–757.
- Page, E. S. (1954). Continuous inspection schemes. *Biometrika* 41(1/2), 100–115.
- Pentland, A., N. Eagle, and D. Lazer (2009). Inferring social network structure using mobile phone data. *Proceedings of the National Academy of Sciences (PNAS)* 106(36), 15274–15278.
- Rand, W. M. (1971). Objective criteria for the evaluation of clustering methods. *Journal of the American Statistical Association* 66(336), 846–850.
- Rice, G. and C. Zhang (2019). Consistency of binary segmentation for multiple change-points estimation with functional data. *arXiv:2001.00093*.
- Rosenbaum, P. R. (2005). An exact distribution-free test comparing two multivariate distributions based on adjacency. *Journal of the Royal Statistical Society: Series B (Statistical Methodology)* 67(4), 515–530.
- Sejdinovic, D., B. Sriperumbudur, A. Gretton, and K. Fukumizu (2013). Equivalence of distance-based and rkhs-based statistics in hypothesis testing. *The Annals of Statistics*, 2263–2291.
- Sinn, M., A. Ghodsi, and K. Keller (2012). Detecting change-points in time series by maximum mean discrepancy of ordinal pattern distributions. *arXiv:1210.4903*.
- Song, H. and H. Chen (2020). Asymptotic distribution-free change-point detection for data with repeated observations. *arXiv:2006.10305*.
- Talih, M. and N. Hengartner (2005). Structural learning with time-varying components: tracking the cross-section of financial time series. *Journal of the Royal Statistical Society: Series B (Statistical Methodology)* 67(3), 321–341.

Tewes, J. (2017). *Change-point tests and the bootstrap under long-and short-range dependence*. Ph. D. thesis, Ruhr-Universität Bochum.

Vavrek, M. (2015). Fossil: palaeoecological and palaeogeographical analysis tools. r package version 0.3. 7.

A Additional Theoretical Results

Proposition 1. \tilde{k} defined in Equation (13) does not depend on centering point y_0 .

Proof. For any kernel $k^{(y_0)}$ induced from d , from the Moore-Aronszajn Theorem (Berlinet and Thomas-Agnan, 2011), there exists an RKHS \mathcal{H}_k with reproducing kernel $k^{(y_0)}$. We call $\phi^{(y_0)} : y \mapsto k^{(y_0)}(\cdot, y)$ the feature map of $k^{(y_0)}$. Notice $\langle \phi^{(y_0)}(y_i), \phi^{(y_0)}(y_j) \rangle_{\mathcal{H}_k} = k^{(y_0)}(y_i, y_j)$. From Lemma 3.1, for different centering points y_0 and y'_0 , if $\phi^{(y_0)}(\cdot)$ is a feature map for $k^{(y_0)}$, then $\phi^{(y'_0)}$ defined as $\phi^{(y'_0)}(y) = \phi^{(y_0)}(y) - \phi^{(y_0)}(y'_0)$ is a feature map for $k^{(y'_0)}$. This implies $\phi^{(y'_0)}(y) - \mathbb{E}\phi^{(y'_0)}(y) = \phi^{(y_0)}(y) - \mathbb{E}\phi^{(y_0)}(y)$ for any y_0, y'_0 and thus, by definition, \tilde{k} does not depend on y_0 . □

Proposition 2. Under the null, if $\forall l \in \mathbb{Z}_+$, $\mathbb{E} [\|\phi(y) - \mathbb{E}\phi(y)\|_{\mathcal{H}}^2 (\phi_l(y) - \mathbb{E}\phi_l(y))] = 0$ holds, then S_1 and S_2 are asymptotically independent.

Proof. See Section B.7. □

Remark A.1. Notice that if $y_i \in \mathbb{R}^p$, each coordinate of y_i is independent and follows a symmetric distribution, and d is defined as the Euclidean distance, Proposition 2 shows that S_1 and S_2 are asymptotically independent.

B Technical Proofs

This section includes proofs to all theoretical results in the main text. First, let us introduce some additional notations.

B.1 Additional Notations

Denote F^i as the distribution that y_i follows, i.e., $F^i = F_0$ for all i under the null and $F^i = F_k$ for $i = \tau_k^* + 1, \dots, \tau_{k+1}^*$ under the alternative. We denote $z_i = \phi(y_i)$, $\mu^i = \mathbb{E}_{F^i}\phi(Y)$, and $\epsilon_i = z_i - \mu^i$. Denote $\bar{\epsilon}_n = \frac{1}{n} \sum_{i=1}^n \epsilon_i$, $\bar{\epsilon}_{t-} = \frac{1}{t} \sum_{i=1}^t \epsilon_i$ and $\bar{\epsilon}_{t+} = \frac{1}{n-t} \sum_{i=t+1}^n \epsilon_i$.

Define $(\boldsymbol{\mu}^*)_{t-} = (\mu^1, \mu^2, \dots, \mu^t)^\top \in \mathcal{H}^t$, $(\boldsymbol{\mu}^*)_{t+} = (\mu^{t+1}, \mu^{t+2}, \dots, \mu^n)^\top \in \mathcal{H}^{n-t}$, $(\boldsymbol{\mu})_{t-} = (\bar{\mu}_{t-}, \bar{\mu}_{t-}, \dots, \bar{\mu}_{t-})^\top \in \mathcal{H}^t$ where $\bar{\mu}_{t-} = \frac{1}{t} \sum_{i=1}^t \mu^i$, and $(\boldsymbol{\mu})_{t+} = (\bar{\mu}_{t+}, \bar{\mu}_{t+}, \dots, \bar{\mu}_{t+})^\top \in \mathcal{H}^{n-t}$ where $\bar{\mu}_{t+} = \frac{1}{n-t} \sum_{i=t+1}^n \mu^i$. The norm in spaces \mathcal{H}^t and \mathcal{H}^{n-t} are defined in the same way as that in \mathcal{H} . Let $s^2 = \lim_{n \rightarrow \infty} \frac{1}{n} \sum_{i=1}^n \text{Var}_{F^i}(\|\phi(Y) - \frac{1}{n} \sum_{i=1}^n \mu^i\|^2)$. Notice that $s^2 = \text{Var}_{F_0}(\|\epsilon\|^2)$ if there is no change point. Write $\boldsymbol{\epsilon}_{t-} = (\epsilon_1, \dots, \epsilon_t)^\top$, and $\boldsymbol{\epsilon}_{t+} = (\epsilon_{t+1}, \dots, \epsilon_n)^\top$. We define the operator Π as $\Pi(\boldsymbol{\epsilon}_{t-}) = \arg \min_{f=(f_1, f_2, \dots, f_t) \in \mathcal{H}^t, f_1=f_2=\dots=f_t} \{\|f - (\boldsymbol{\epsilon})_{t-}\|^2\}$. From Appendix A.1 of [Arlot et al. \(2012\)](#), we know that $\Pi(\boldsymbol{\epsilon}_{t-}) = (\bar{\epsilon}_{t-}, \bar{\epsilon}_{t-}, \dots, \bar{\epsilon}_{t-})^\top$. We use \xrightarrow{p} to denote convergence in probability.

B.2 Some Useful Results

The following are some useful results which will be utilized in later proofs.

Lemma B.1 (Proposition 1 from [Arlot et al. \(2012\)](#)). *If (1) $\exists M > 0$ such that $\forall i \in \{1, 2, \dots, n\}$, $\|\tilde{k}(y_i, y_i)\|^2 \leq M^2$, a.s. (2) y_i 's are independent, then, for any $x > 0$,*

$$\mathbb{P} \left(\left| \frac{1}{n} \left\| \sum_{i=1}^n \epsilon_i \right\|^2 - \frac{1}{n} \mathbb{E} \left\| \sum_{i=1}^n \epsilon_i \right\|^2 \right| \leq \frac{14M^2}{3} (x + 2\sqrt{2x}) \right) \geq 1 - 2e^{-x}.$$

From Equation (19) in [Arlot et al. \(2012\)](#), $\frac{1}{n} \mathbb{E} \left\| \sum_{i=1}^n \epsilon_i \right\|^2 \leq CM^2$ where C is the number of change points +1. Thus, we have

$$\mathbb{P} \left(\frac{1}{\sqrt{n}} \left\| \sum_{i=1}^n \epsilon_i \right\| \leq \sqrt{CM^2 + \frac{14M^2}{3} (x + 2\sqrt{2x})} \right) \geq 1 - 2e^{-x}. \quad (29)$$

Lemma B.2 (Lemma 7.10 from [Garreau et al. \(2018\)](#)). *If (1) there exists a positive constant V s.t. $\max_{1 \leq i \leq n} \mathbb{E} \|\epsilon_i\|^2 \leq V$, (2) y_i 's are independent, then, for any $x > 0$,*

$$\mathbb{P} \left(\left\| \sum_{i=1}^n \epsilon_i \right\| \leq e^{x/2} \sqrt{nV} \right) \geq 1 - e^{-x}.$$

Now we are ready to present proofs of the results in the main article.

B.3 Proof of Theorem 4.1

B.3.1 On S_1

Conclusion (a) is a direct consequence of the following Lemma:

Lemma B.3. *Under the null, if*

(1) *d is a semi-metric of negative type, and*

(2) $\mathbb{E}_y \left| \tilde{k}(y, y) \right|^{2+\delta} < +\infty$ *for some $\delta > 0$,*

(3) $\mathbb{E}_{y, y'} \left| \tilde{k}(y, y') \right|^2 < \infty$,

then for any $0 < \rho < 1$, as $n \rightarrow \infty$, we have

$$n\rho^2(1-\rho)^2 \left(\bar{d}_{A(\lceil n\rho \rceil)} - \frac{1}{2} \bar{d}_{B_1(\lceil n\rho \rceil)} - \frac{1}{2} \bar{d}_{B_2(\lceil n\rho \rceil)} \right) \xrightarrow{w} \sum_{l=1}^{\infty} \lambda_l (W_l^0(\rho)^2 - \rho(1-\rho)),$$

where $W_l^0(\cdot)$'s are independent Brownian bridges, λ_l 's are eigenvalues of \tilde{k} defined in Equation (14).

Proof. From assumption (1), we know that Lemma 3.1 holds. Together with assumption (3), we know that eigen-decomposition (14) holds.

Notice that assumption (2) is equivalent to $\mathbb{E} \|\phi(y)\|^{4+2\delta} < \infty$. Since our data are i.i.d under the null, from Theorem 16 in Tewes (2017), by directly treating $\{\phi(y_i)\}$ as the observations in Hilbert space \mathcal{H} , we have

$$\frac{1}{\sqrt{n}} \sum_{i=1}^{\lceil n\rho \rceil} (\phi(y_i) - \mu) \xrightarrow{w} \mathbf{W}(\rho),$$

where $\mathbf{W}(\rho)$ is a Brownian motion in \mathcal{H} and $\mathbf{W}(1)$ has the covariance operator $\Sigma: \mathcal{H} \rightarrow \mathcal{H}$, defined by

$$\langle \Sigma\phi(y), \phi(y') \rangle = \mathbb{E}_{y''} [\langle \phi(y'') - \mathbb{E}\phi(y''), \phi(y') \rangle \langle \phi(y'') - \mathbb{E}\phi(y''), \phi(y') \rangle], \quad \forall y, y' \in \mathcal{H}.$$

From the definition of $\phi(\cdot)$ and \tilde{k} in Section 3.3, we have

$$\langle \Sigma\phi(y), \phi(y') \rangle = \mathbb{E}_{y''} \sum_{l,m} \phi_l(y) \phi_m(y') [\phi_l(y'') \phi_m(y'')] = \sum_l \lambda_l \phi_l(y) \phi_l(y'),$$

as long as the last quantity is well-defined. Thus, we know $\mathbf{W}(\rho) = (\sqrt{\lambda_1}W_1(\rho), \sqrt{\lambda_2}W_2(\rho), \dots)^\top$ where $W_l(\rho)$ and $W_m(\rho)$ are independent Brownian motions if $l \neq m$. Thus, a direct consequence of Corollary 5.2.1 in Tewes (2017) is that

$$\frac{1}{n} \left\| \frac{n-t}{n} \sum_{i=1}^t \phi(y_i) - \frac{t}{n} \sum_{i=t+1}^n \phi(y_i) \right\|^2 \xrightarrow{w} \|\mathbf{W}(\rho) - \rho\mathbf{W}(1)\|^2 = \sum_l \lambda_l W_l^0(\rho)^2, \quad (30)$$

where $t = \lceil n\rho \rceil$.

After some tedious calculations, we know

$$\begin{aligned}
& \frac{1}{n} \left\| \frac{n-t}{n} \sum_{i=1}^t \phi(y_i) - \frac{t}{n} \sum_{i=t+1}^n \phi(y_i) \right\|^2 = \frac{(n-t)^2 t^2}{n^3} \left[\frac{1}{t(n-t)} d_{A(t)} - \frac{1}{2t^2} d_{B_1(t)} - \frac{1}{2(n-t)^2} d_{B_2(t)} \right] \\
&= \frac{(n-t)^2 t^2}{n^3} \left[\frac{1}{t(n-t)} d_{A(t)} - \frac{1}{2t(t-1)} d_{B_1(t)} - \frac{1}{2(n-t)^2} d_{B_2(t)} \right] + \frac{(n-t)^2}{2n^3(t-1)} d_{B_1(t)} + \frac{t^2}{2n^3(n-t-1)} d_{B_1(t)} \\
&\stackrel{(a)}{=} n\rho^2(1-\rho)^2 \left[\bar{d}_{A(\lceil n\rho \rceil)} - \frac{1}{2} \bar{d}_{B_1(\lceil n\rho \rceil)} - \frac{1}{2} \bar{d}_{B_2(\lceil n\rho \rceil)} \right] + \frac{(n-t)^2 t}{n^3(t-1)} \sum_{i=1}^t \|\hat{\epsilon}_i\|^2 + \frac{t^2(n-t)}{n^3(n-t-1)} \sum_{i=t+1}^n \|\hat{\epsilon}_i\|^2,
\end{aligned} \tag{31}$$

where $\hat{\epsilon}_i = \phi(y_i) - \bar{\phi}(y)_{t-}$ for $i = 1, 2, \dots, t$ and $\hat{\epsilon}_i = \phi(y_i) - \bar{\phi}(y)_{t+}$ for $i = t+1, t+2, \dots, n$. Here (a) follows from the fact that $d_{B_1(t)} = 2t \sum_{i=1}^t \|\epsilon_i - \bar{\epsilon}_{t-}\|^2$ and $d_{B_2(t)} = 2(n-t) \sum_{i=t+1}^n \|\epsilon_i - \bar{\epsilon}_{t+}\|^2$.

Since $t \rightarrow \infty, n-t \rightarrow \infty$ as $n \rightarrow \infty$, we know that

$$\begin{aligned}
\frac{1}{t} \sum_{i=1}^t \|\hat{\epsilon}_i\|^2 - \mathbb{E}\|\epsilon\|^2 &= \frac{1}{t} \sum_{i=1}^t (\|\hat{\epsilon}_i\|^2 - \|\epsilon_i\|^2) + \frac{1}{t} \sum_{i=1}^t \|\epsilon_i\|^2 - \mathbb{E}\|\epsilon\|^2 \\
&= \left\| \frac{1}{t} \sum_{i=1}^t \epsilon_i \right\|^2 + \frac{1}{t} \sum_{i=1}^t (\|\epsilon_i\|^2 - \mathbb{E}\|\epsilon\|^2) \xrightarrow{p} 0,
\end{aligned} \tag{32}$$

where the convergence in probability follows from Lemma B.2 and law of large numbers (assumption 2 implies the boundedness of $\text{Var}(\|\epsilon_i\|^2)$). Similarly we have

$$\frac{1}{n-t} \sum_{i=t+1}^n \|\hat{\epsilon}_i\|^2 - \mathbb{E}\|\epsilon\|^2 = \frac{1}{n-t} \sum_{i=t+1}^n (\|\hat{\epsilon}_i\|^2 - \|\epsilon_i\|^2) + \frac{1}{n-t} \sum_{i=t+1}^n \|\epsilon_i\|^2 - \mathbb{E}\|\epsilon\|^2 \xrightarrow{p} 0. \tag{33}$$

Since $\mathbb{E}\|\epsilon\|^2 = \sum_l \lambda_l$, combining Equation (30), (31), (32) and (33), we have

$$n\rho^2(1-\rho)^2 \left[\bar{d}_{A(\lceil n\rho \rceil)} - \frac{1}{2} \bar{d}_{B_1(\lceil n\rho \rceil)} - \frac{1}{2} \bar{d}_{B_2(\lceil n\rho \rceil)} \right] \xrightarrow{w} \sum_l \lambda_l (W_l^0(\rho)^2 - \rho(1-\rho)).$$

Now we want to make sure that $\sum_l \lambda_l (W_l^0(\rho)^2 - \rho(1-\rho))$ is well defined. Notice that

$$\begin{aligned}
& \mathbb{E} \left[\sum_l \lambda_l (W_l^0(\rho)^2 - \rho(1-\rho)) \right] = 0, \\
& \text{Var} \left(\sum_l \lambda_l (W_l^0(\rho)^2 - \rho(1-\rho)) \right) = 2 \sum_l \lambda_l^2 (1-\rho)^2 \rho^2 \stackrel{(b)}{<} +\infty,
\end{aligned}$$

where (b) follows from assumption (3) because assumption (3) is equivalent to

$$\int_y \int_{y'} \tilde{k}(y, y') dF_0(y) dF_0(y') < +\infty,$$

which implies that $\sum_l \lambda_l^2 < +\infty$. □

B.3.2 On S_2

Conclusion (b) is a direct consequence of Lemma B.4.

Lemma B.4. *Under the null, if distance d satisfies*

- (1) d is a semi-metric of negative type,
 - (2) $\mathbb{E}_y \tilde{k}(y, y) \leq M^2$, and
 - (3) $\mathbb{E}_y |\tilde{k}(y, y) - \mathbb{E}_y \tilde{k}(y, y)|^{2+\delta} < +\infty$ for some $\delta > 0$,
- then, for any $0 < \rho < 1$,

$$\frac{\sqrt{n}\rho(1-\rho)}{2\widehat{s}_n} (\bar{d}_{B_1(\lceil n\rho\rceil)} - \bar{d}_{B_2(\lceil n\rho\rceil)}) \xrightarrow{w} W^0(\rho), \quad n \rightarrow \infty. \quad (34)$$

Proof. The proof is similar to the proof of Theorem 2.1 in Lee et al. (2003). Write $t = \lceil n\rho \rceil$.

$$\begin{aligned} & \frac{1}{\sqrt{n}\widehat{s}_n} \frac{t(n-t)}{2n} (\bar{d}_{B_1(t)} - \bar{d}_{B_2(t)}) = \frac{1}{\sqrt{n}} \frac{s_n}{\widehat{s}_n} \frac{1}{s_n} \left[\frac{t}{t-1} \frac{n-t}{n} \sum_{i=1}^t \|\epsilon_i\|^2 - \frac{n-t}{n-t-1} \frac{t}{n} \sum_{i=t+1}^n \|\epsilon_i\|^2 \right] \\ & + \frac{1}{\widehat{s}_n} \frac{1}{\sqrt{n}} \frac{t}{t-1} \frac{n-t}{n} \sum_{i=1}^t (\|z_i - \bar{z}_{t-}\|^2 - \|\epsilon_i\|^2) - \frac{1}{\widehat{s}_n} \frac{1}{\sqrt{n}} \frac{n-t}{n-t-1} \frac{t}{n} \sum_{i=t+1}^n (\|z_i - \bar{z}_{t+}\|^2 - \|\epsilon_i\|^2) \\ & = U_1 + U_2 + U_3, \end{aligned}$$

where

$$\begin{aligned} U_1 &= \frac{1}{\sqrt{n}} \frac{s_n}{\widehat{s}_n} \frac{1}{s_n} \left[\frac{t}{t-1} \frac{n-t}{n} \sum_{i=1}^t \|\epsilon_i\|^2 - \frac{n-t}{n-t-1} \frac{t}{n} \sum_{i=t+1}^n \|\epsilon_i\|^2 \right], \\ U_2 &= \frac{1}{\widehat{s}_n} \frac{1}{\sqrt{n}} \frac{t}{t-1} \frac{n-t}{n} \sum_{i=1}^t (\|z_i - \bar{z}_{t-}\|^2 - \|\epsilon_i\|^2), \\ U_3 &= -\frac{1}{\widehat{s}_n} \frac{1}{\sqrt{n}} \frac{n-t}{n-t-1} \frac{t}{n} \sum_{i=t+1}^n (\|z_i - \bar{z}_{t+}\|^2 - \|\epsilon_i\|^2). \end{aligned}$$

Now we derive the asymptotic property of each of them separately.

First we show that $U_1 \xrightarrow{w} W^0(\rho)$. Notice that assumption (3) in Lemma B.4 implies $\mathbb{E}|\|\epsilon\|^2 - \mathbb{E}\|\epsilon\|^2|^{2+\delta} < +\infty$ for some $\delta > 0$. Thus, by treating $\|\epsilon_i\|$ as a (univariate) variable, it is a direct consequence from Lemma 3.1 of Doukhan (2012) that

$$\frac{1}{\sqrt{ns}} \left[\frac{t}{t-1} \frac{n-t}{n} \sum_{i=1}^t \|\epsilon_i\|^2 - \frac{n-t}{n-t-1} \frac{t}{n} \sum_{i=t+1}^n \|\epsilon_i\|^2 \right] \xrightarrow{w} W^0(\rho).$$

Combined with Lemma B.5, we know that $U_1(t) \xrightarrow{w} W^0(\rho)$.

Then we show that $U_2 \xrightarrow{P} 0$. Notice that

$$U_2 = \frac{1}{\sqrt{n}} \sum_{i=1}^t (\|z_i - \bar{z}_{t-}\|^2 - \|\epsilon_i\|^2) = \frac{1}{\sqrt{n}} \sum_{i=1}^t (\|\epsilon_i - \bar{\epsilon}_{t-}\|^2 - \|\epsilon_i\|^2) = -\frac{1}{\sqrt{n}} \frac{1}{t} \sum_{i=1}^t \epsilon_i \xrightarrow{P} 0,$$

where the convergence in probability follows Lemma B.2.

The fact that $U_3 \xrightarrow{P} 0$ can be proved in a similar way.

To sum, this means

$$\frac{1}{\sqrt{ns}} \frac{t(n-t)}{2n} (\bar{d}_{B_1(t)} - \bar{d}_{B_2(t)}) \xrightarrow{w} W^0(\rho).$$

From Lemma B.5, we have

$$\frac{\widehat{s}_n}{s} \xrightarrow{P} 1.$$

Thus,

$$\frac{1}{\sqrt{n\widehat{s}_n}} \frac{t(n-t)}{2n} (\bar{d}_{B_1(t)} - \bar{d}_{B_2(t)}) \xrightarrow{w} W^0(\rho).$$

□

Lemma B.5. *Suppose d is a semi-metric of negative type. If there exists a positive constant M s.t. $\max_{1 \leq i \leq n} \mathbb{E}_{F^i} \left(\widetilde{k}(y, y) - \mathbb{E}_{F^i} \widetilde{k}(y, y) \right)^2 \leq M^2$, we have that $\widehat{s}_n \xrightarrow{P} s$.*

Remark B.1. *Notice that this Lemma holds for both the alternative and the null.*

Proof. The proof follows from proof of Lemma 3.3 in Lee et al. (2003). Notice that $\widehat{s}_n^2 = \frac{1}{n} \sum_{i=1}^n (\|\hat{\epsilon}_i\|^2 - \hat{m}_n)^2$ where $\hat{m}_n = \frac{1}{n} \sum_{i=1}^n \|\hat{\epsilon}_i\|^2$ and $\hat{\epsilon}_i = z_i - \bar{z}$. Denote $\tilde{\epsilon}_i = z_i - \frac{1}{n} \sum_{i=1}^n \mu^i$, $\tilde{m}_n = \frac{1}{n} \sum_{i=1}^n \|\tilde{\epsilon}_i\|^2$. Denote $\widetilde{s}_n^2 = \frac{1}{n} \sum_{i=1}^n (\|\tilde{\epsilon}_i\|^2 - \tilde{m}_n)^2$. Notice that $\hat{\epsilon}_i = \tilde{\epsilon}_i - \bar{\epsilon}_n$. Notice that $\mathbb{E}\|\epsilon_i\|^2 \leq M^2$ is equivalent to $\mathbb{E}\|\phi(y_i)\|^2 \leq M^2$.

Notice that

$$\begin{aligned}
\widehat{s}_n^2 &= \frac{1}{n} \sum_{i=1}^n (\|\hat{\epsilon}_i\|^2 - \|\tilde{\epsilon}_i\|^2 + \|\tilde{\epsilon}_i\|^2 - \tilde{m}_n + \tilde{m}_n - \hat{m}_n)^2 \\
&= \frac{1}{n} \sum_{i=1}^n (\|\tilde{\epsilon}_i\|^2 - \tilde{m}_n)^2 + (\|\hat{\epsilon}_i\|^2 - \|\tilde{\epsilon}_i\|^2)^2 + (\tilde{m}_n - \hat{m}_n)^2 \\
&\quad + 2(\|\hat{\epsilon}_i\|^2 - \|\tilde{\epsilon}_i\|^2)(\|\tilde{\epsilon}_i\|^2 - \tilde{m}_n) + 2(\|\hat{\epsilon}_i\|^2 - \|\tilde{\epsilon}_i\|^2)(\tilde{m}_n - \hat{m}_n) + 2(\|\tilde{\epsilon}_i\|^2 - \tilde{m}_n)(\tilde{m}_n - \hat{m}_n) \\
&= \widetilde{s}_n^2 + R_1 + R_2 + 2R_3 + 2R_4 + 2R_5,
\end{aligned}$$

where

$$\begin{aligned}
R_1 &= \frac{1}{n} \sum_{i=1}^n (\|\hat{\epsilon}_i\|^2 - \|\tilde{\epsilon}_i\|^2)^2, \quad R_2 = \frac{1}{n} \sum_{i=1}^n (\tilde{m}_n - \hat{m}_n)^2, \quad R_3 = \frac{1}{n} \sum_{i=1}^n 2(\|\hat{\epsilon}_i\|^2 - \|\tilde{\epsilon}_i\|^2)(\|\tilde{\epsilon}_i\|^2 - \tilde{m}_n), \\
R_4 &= \frac{1}{n} \sum_{i=1}^n 2(\|\hat{\epsilon}_i\|^2 - \|\tilde{\epsilon}_i\|^2)(\tilde{m}_n - \hat{m}_n), \quad R_5 = \frac{1}{n} \sum_{i=1}^n 2(\|\tilde{\epsilon}_i\|^2 - \tilde{m}_n)(\tilde{m}_n - \hat{m}_n).
\end{aligned}$$

Now we bound each of them separately. Firstly,

$$\begin{aligned}
R_1 &= \frac{1}{n} \sum_{i=1}^n (\|\hat{\epsilon}_i\|^2 - \|\tilde{\epsilon}_i\|^2)^2 = \frac{1}{n} \sum_{i=1}^n (\|\tilde{\epsilon}_i - \bar{\epsilon}_n\|^2 - \|\tilde{\epsilon}_i\|^2)^2 \\
&= \frac{1}{n} \sum_{i=1}^n (\|\bar{\epsilon}_n\|^2 + 2\langle \tilde{\epsilon}_i, \bar{\epsilon}_n \rangle)^2 \leq \frac{1}{n} \sum_{i=1}^n [2\|\bar{\epsilon}_n\|^4 + 2(2\langle \tilde{\epsilon}_i, \bar{\epsilon}_n \rangle)^2] \\
&\leq 2\|\bar{\epsilon}_n\|^4 + \left(\frac{8}{n} \sum_{i=1}^n \|\tilde{\epsilon}_i\|^2 \right) \times \|\bar{\epsilon}_n\|^2.
\end{aligned}$$

Since

$$\begin{aligned}
\frac{1}{n} \sum_{i=1}^n \|\tilde{\epsilon}_i\|^2 &\xrightarrow{p} \mathbb{E}\|\tilde{\epsilon}_i\|^2, \quad \text{where} \\
\mathbb{E}\|\tilde{\epsilon}_i\|^2 &= \mathbb{E} \left\| \mu^i - \frac{1}{n} \sum_{i=1}^n \mu^i + \epsilon_i \right\|^2 = \mathbb{E} \left\| \phi(y_i) - \frac{1}{n} \sum_{i=1}^n \mu^i \right\|^2 \leq 2\mathbb{E} \left\| \phi(y_i) \right\|^2 + 2\mathbb{E} \left\| \frac{1}{n} \sum_{i=1}^n \mu^i \right\|^2 \\
&\leq 2\mathbb{E} \left\| \phi(y_i) \right\|^2 + 2\mathbb{E} \left\| \frac{1}{n} \sum_{i=1}^n (\mu^i + \epsilon_i) \right\|^2 \leq C,
\end{aligned}$$

and $\|\bar{\epsilon}_n\| \xrightarrow{p} 0$ (Lemma B.2), we have $R_1 \xrightarrow{p} 0$. Then,

$$R_2 = \left(\frac{1}{n} \sum_{i=1}^n \|\hat{\epsilon}_i\|^2 - \frac{1}{n} \sum_{i=1}^n \|\tilde{\epsilon}_i\|^2 \right)^2 = \left(\frac{1}{n} \sum_{i=1}^n \|\bar{\epsilon}_n\|^2 + \left\langle \frac{2}{n} \sum_{i=1}^n \epsilon_i, -\bar{\epsilon}_n \right\rangle \right)^2 = \|\bar{\epsilon}_n\|^4.$$

Since $\|\bar{\epsilon}_n\| \xrightarrow{p} 0$, we have $R_2 \xrightarrow{p} 0$. Then,

$$\begin{aligned} |R_3| &= \left| \frac{1}{n} \sum_{i=1}^n (\|\hat{\epsilon}_i\|^2 - \|\tilde{\epsilon}_i\|^2)(\|\tilde{\epsilon}_i\|^2 - \tilde{m}_n) \right| \\ &\leq \sqrt{\frac{1}{n} \sum_{i=1}^n (\|\hat{\epsilon}_i\|^2 - \|\tilde{\epsilon}_i\|^2)^2 \frac{1}{n} \sum_{i=1}^n (\|\tilde{\epsilon}_i\|^2 - \tilde{m}_n)^2} \\ &\leq \sqrt{R_1 \left(\frac{1}{n} \sum_{i=1}^n \|\tilde{\epsilon}_i\|^4 - \tilde{m}_n^2 \right)} = \sqrt{R_1 \tilde{s}_n^2}. \end{aligned}$$

Recall that when there is no change point, we have $\rho^* = 1$. Then, from Law of Large Numbers, we have

$$\tilde{s}_n^2 = \frac{1}{n} \sum_{i=1}^n \|\tilde{\epsilon}_i\|^4 - \tilde{m}_n^2 \xrightarrow{p} s^2, \quad (35)$$

where s^2 is a bounded positive constant because for any i ,

$$\begin{aligned} \text{Var}_{F^i} \left(\left\| \phi(y) - \frac{1}{n} \sum_{i=1}^n \mu^i \right\|^2 \right) &= \mathbb{E}_{F^i} \left(\|\phi(y)\|^2 - \mathbb{E}_{F^i} \|\phi(y)\|^2 - 2 \left\langle \frac{1}{n} \sum_{i=1}^n \mu^i, \epsilon \right\rangle \right)^2 \\ &\leq 2\mathbb{E}_{F^i} (\|\phi(y)\|^2 - \mathbb{E}_{F^i} \|\phi(y)\|^2)^2 + 2\mathbb{E}_{F^i} \left(2 \left\langle \frac{1}{n} \sum_{i=1}^n \mu^i, \epsilon \right\rangle \right)^2 \\ &\leq 2\mathbb{E}_{F^i} \left(\tilde{k}(y, y) - \mathbb{E}_{F^i} \tilde{k}(y, y) \right)^2 + 8\mathbb{E}_{F^i} \|\epsilon\|^2 \left(\frac{1}{n} \sum_{i=1}^n \|\mu^i\| \right)^2 \\ &\stackrel{(a)}{\leq} 2\mathbb{E}_{F^i} \left(\tilde{k}(y, y) - \mathbb{E}_{F^i} \tilde{k}(y, y) \right)^2 + 8\mathbb{E}_{F^i} \tilde{k}(y, y) \frac{1}{n} \sum_{i=1}^n \|\mu^i\|^2 < +\infty. \end{aligned}$$

where (a) follows from the fact that $\mathbb{E}_{F^i} \|\epsilon\|^2 = \mathbb{E}_{F^i} \|\phi(Y) - \mathbb{E}_{F^i} \phi(Y)\|^2 \leq \mathbb{E}_{F^i} \|\phi(Y)\|^2 = \mathbb{E}_{F^i} \tilde{k}(y, y)$, and $\left(\frac{1}{n} \sum_{i=1}^n \|\mu^i\| \right)^2 \leq \frac{1}{n} \sum_{i=1}^n \|\mu^i\|^2 = \frac{1}{n} \sum_{i=1}^n \|\mathbb{E}_{F^i} \phi(Y)\|^2 \leq \frac{1}{n} \sum_{i=1}^n \mathbb{E}_{F^i} \|\phi(Y)\|^2 = \frac{1}{n} \sum_{i=1}^n \mathbb{E}_{F^i} \tilde{k}(Y, Y)$. Combined with $R_1 \xrightarrow{p} 0$, we have $R_3 \xrightarrow{p} 0$.

$$|R_4| = \left| \frac{2}{n} \sum_{i=1}^n (\|\hat{\epsilon}_i\|^2 - \|\epsilon_i\|^2)(\tilde{m}_n - \hat{m}_n) \right| = 2|\tilde{m}_n - \hat{m}_n| \times \left| \frac{1}{n} \sum_{i=1}^n \|\hat{\epsilon}_i\|^2 - \mathbb{E} \|\epsilon_i\|^2 \right| \xrightarrow{p} 0,$$

where the convergence in probability follows from the fact that $R_2 = (\tilde{m}_n - \hat{m}_n)^2 \xrightarrow{p} 0$, and $\frac{1}{n} \sum_{i=1}^n \|\hat{\epsilon}_i\|^2 - \mathbb{E} \|\epsilon_i\|^2 \xrightarrow{p} 0$ (law of large numbers).

$$|R_5| = \left| \frac{1}{n} \sum_{i=1}^n (\|\epsilon_i\|^2 - \tilde{m}_n)(\tilde{m}_n - \hat{m}_n) \right| = 0,$$

where the last equality follows from the definition of \tilde{m}_n .

Combining the above, we know that $\widehat{s}_n - \tilde{s}_n \xrightarrow{P} 0$ and thus, $\frac{\tilde{s}_n}{\widehat{s}_n} \xrightarrow{P} 1$. Equation (35) says $\tilde{s}_n \xrightarrow{P} s^2$. Thus, we have $\widehat{s}_n \xrightarrow{P} s^2$. This completes the proof. \square

B.4 Proof of Theorem 4.2

Conclusion (1) is a direct consequence of Theorem B.1 and (2) is a direct consequence of Theorem B.2 .

Theorem B.1 (Alternative distribution for S_1). *In AMOC setting, under the alternative, if (1) d is a semi-metric of negative type, (2) there exists positive constant M such that for all $i \in \{1, 2, \dots, n\}$, $\tilde{k}(y_i, y_i) \leq M^2$ a.s., (3) there exists $\Delta^{(1)} \in \mathcal{H}$ s.t. $\|\sqrt{n}(\mu_0 - \mu_1) - \Delta^{(1)}\| \rightarrow 0$, then*

$$S_1 \xrightarrow{w} \max_{\rho \in [\rho_0, \rho_1]} \left(\frac{\sum_l \left(\sqrt{\lambda_l} W^0(\rho) + \xi(\rho) \Delta_l^{(1)} \right)^2 - \delta(\rho)}{\rho(1-\rho)} \right),$$

where

$$\delta(\rho) = \begin{cases} (1-\rho) \left((1-\rho)\rho^* v_0 + (\rho - \rho^* + \rho\rho^*) v_1 \right), & \text{if } \rho^* \leq \rho \\ \rho(\rho(1-\rho^*)v_1 + (\rho\rho^* - 2\rho + 1)v_0), & \text{if } \rho^* > \rho \end{cases},$$

and

$$\xi(\rho) = \begin{cases} \rho(1-\rho^*), & \text{if } \rho \leq \rho^* \\ (1-\rho)\rho^*, & \text{if } \rho > \rho^* \end{cases}.$$

Theorem B.2 (Alternative distribution for S_2). *In AMOC setting, under the alternative, if (1) d is a semi-metric of negative type, (2) there exists positive constant M such that for all $i \in \{1, 2, \dots, n\}$, $\tilde{k}(y_i, y_i) \leq M^2$ a.s., (3) $\sqrt{n}(v_0 - v_1) \rightarrow \Delta_v^{(2)}$ and (4) $\sqrt{n}\|\mu_0 - \mu_1\|^2 \rightarrow \Delta_\mu^{(2)}$, then*

$$S_2 \xrightarrow{w} \max_{\rho \in [\rho_0, \rho_1]} \left(\frac{|G + \Delta^{(2)}|}{\sqrt{\rho(1-\rho)}} \right),$$

where G is some Gaussian process and

$$\Delta^{(2)} = \begin{cases} \frac{1}{s}\rho^*(1-\rho) \left(\Delta_v^{(2)} + \frac{\rho-\rho^*}{\rho} \Delta_\mu^{(2)} \right), & \rho \geq \rho^* \\ \frac{1}{s}(1-\rho^*)\rho \left(\Delta_v^{(2)} - \frac{\rho^*-\rho}{1-\rho} \Delta_\mu^{(2)} \right), & \rho < \rho^* \end{cases}.$$

B.4.1 Proof of Theorem B.1

Proof. Denote $t = \lceil n\rho \rceil$. For each $\rho \in [\rho_0, \rho_1]$, we show that

$$n\rho^2(1-\rho)^2 \left[\bar{d}_{A(\lceil n\rho \rceil)} - \frac{1}{2}\bar{d}_{B_1(\lceil n\rho \rceil)} - \frac{1}{2}\bar{d}_{B_2(\lceil n\rho \rceil)} \right] \xrightarrow{w} \frac{\sum_l \left(\sqrt{\lambda_l} W^0(\rho) + \xi(\rho) \Delta_l^{(1)} \right)^2 - \delta(\rho)}{\rho(1-\rho)}. \quad (36)$$

In order to show Equation (36), we utilize the following relationship:

$$\begin{aligned} & n\rho^2(1-\rho)^2 \left[\bar{d}_{A(\lceil n\rho \rceil)} - \frac{1}{2}\bar{d}_{B_1(\lceil n\rho \rceil)} - \frac{1}{2}\bar{d}_{B_2(\lceil n\rho \rceil)} \right] \\ &= \frac{1}{n} \left\| \frac{n-t}{n} \sum_{i=1}^t \phi(y_i) - \frac{t}{n} \sum_{i=t+1}^n \phi(y_i) \right\|^2 - \frac{(n-t)^2 t}{n^3(t-1)} \sum_{i=1}^t \|\hat{\epsilon}_i\|^2 - \frac{t^2(n-t)}{n^3(n-t-1)} \sum_{i=t+1}^n \|\hat{\epsilon}_i\|^2 \\ &= U_1 - U_2 - U_3, \end{aligned}$$

where

$$\begin{aligned} U_1 &= \frac{1}{n} \left\| \frac{n-t}{n} \sum_{i=1}^t \phi(y_i) - \frac{t}{n} \sum_{i=t+1}^n \phi(y_i) \right\|^2, \\ U_2 &= \frac{(n-t)^2 t}{n^3(t-1)} \sum_{i=1}^t \|\hat{\epsilon}_i\|^2, \quad U_3 = \frac{t^2(n-t)}{n^3(n-t-1)} \sum_{i=t+1}^n \|\hat{\epsilon}_i\|^2. \end{aligned}$$

and $\hat{\epsilon}_i = \phi(y_i) - \bar{\phi}(y)_{t-}$ for $i = 1, 2, \dots, t$ and $\hat{\epsilon}_i = \phi(y_i) - \bar{\phi}(y)_{t+}$ for $i = t+1, t+2, \dots, n$.

Now we derive asymptotic property for each of U_1, U_2, U_3 separately.

Firstly, from corollary 5.2.2 of [Tewes \(2017\)](#), if $\|\sqrt{n}(\mu_0 - \mu_1) - \mathbf{\Delta}^{(1)}\| \rightarrow 0$, then we have

$$U_1 = \frac{1}{n} \left\| \frac{n-t}{n} \sum_{i=1}^t \phi(y_i) - \frac{t}{n} \sum_{i=t+1}^n \phi(y_i) \right\|^2 \xrightarrow{w} \sum_l \left(\sqrt{\lambda_l} W^0(\rho) + \xi(\rho) \Delta_l^{(1)} \right)^2. \quad (37)$$

Secondly, write $\tilde{\epsilon}_i = z_i - \bar{\mu}_{t-}$ for all $i = 1, 2, \dots, t$, and notice that

$$\begin{aligned}
& \frac{1}{t} \sum_{i=1}^t (\|\hat{\epsilon}_i\|^2 - \mathbb{E}_{F^i} \|\tilde{\epsilon}\|^2) = \frac{1}{t} \sum_{i=1}^t (\|\hat{\epsilon}_i\|^2 - \|\tilde{\epsilon}_i\|^2) + \frac{1}{t} \sum_{i=1}^t (\|\tilde{\epsilon}_i\|^2 - \mathbb{E}_{F^i} \|\tilde{\epsilon}_i\|^2) \\
&= \frac{1}{t} \sum_{i=1}^t (\|\bar{\epsilon}_i\|^2 - 2\langle \mu^i - \bar{\mu}_{t-} + \epsilon_i, \bar{\epsilon}_i \rangle) \\
&\quad + \frac{1}{t} \sum_{i=1}^t [\|\epsilon_i\|^2 + \|\mu^i - \bar{\mu}_{t-}\|^2 + 2\langle \mu^i - \bar{\mu}_{t-}, \epsilon_i \rangle - \mathbb{E}_{F^i} (\|\epsilon_i\|^2 + \|\mu^i - \bar{\mu}_{t-}\|^2 + 2\langle \mu^i - \bar{\mu}_{t-}, \epsilon_i \rangle)] \\
&= -\|\bar{\epsilon}_t\|^2 + \frac{1}{t} \sum_{i=1}^t [\|\epsilon_i\|^2 - \mathbb{E}_{F^i} \|\epsilon_i\|^2] + \frac{1}{t} \sum_{i=1}^t [2\langle \mu^i - \bar{\mu}_{t-}, \epsilon_i \rangle] \xrightarrow{p} 0,
\end{aligned} \tag{38}$$

where the last convergence follows from the fact that $\|\bar{\epsilon}_t\| = \mathcal{O}_p(t^{-1/2})$.

Similarly, denote $\tilde{\epsilon}_i = z_i - \bar{\mu}_{t+}$ for all $i = t+1, \dots, n$, we have

$$\frac{1}{n-t} \sum_{i=t+1}^n (\|\hat{\epsilon}_i\|^2 - \mathbb{E}_{F^i} \|\tilde{\epsilon}\|^2) \xrightarrow{p} 0, \tag{39}$$

Combining Equation (38) and (39), we know that

$$\begin{aligned}
U_2 &\xrightarrow{p} (1-\rho)^2 \rho \lim_{t \rightarrow \infty} \frac{1}{t} \sum_{i=1}^t \mathbb{E}_{F^i} \|z_i - \bar{\mu}_{t-}\|^2 = (1-\rho)^2 \rho \lim_{t \rightarrow \infty} \frac{1}{t} \sum_{i=1}^t [\mathbb{E}_{F^i} \|\epsilon_i\|^2 + \|\mu^i - \bar{\mu}_{t-}\|^2], \\
U_3 &\xrightarrow{p} \rho^2 (1-\rho) \lim_{t \rightarrow \infty} \frac{1}{n-t} \sum_{i=t+1}^n \mathbb{E}_{F^i} \|z_i - \bar{\mu}_{t+}\|^2 = \rho^2 (1-\rho) \lim_{t \rightarrow \infty} \frac{1}{n-t} \sum_{i=t+1}^n [\mathbb{E}_{F^i} \|\epsilon_i\|^2 + \|\mu^i - \bar{\mu}_{t+}\|^2].
\end{aligned}$$

Thus,

$$\begin{aligned}
U_2 + U_3 &\xrightarrow{p} \mathbb{I}(\rho^* \leq \rho) (1-\rho) \left(\rho^* (1-\rho) \frac{\rho - \rho^*}{\rho} \|\mu_0 - \mu_1\|^2 + (1-\rho) \rho^* v_0 + (\rho - \rho^* + \rho \rho^*) v_1 \right) \\
&\quad + \mathbb{I}(\rho^* > \rho) \rho \left(\rho (\rho^* - \rho) \frac{1 - \rho^*}{1 - \rho} \|\mu_0 - \mu_1\|^2 + \rho (1 - \rho^*) v_1 + (\rho \rho^* - 2\rho + 1) v_0 \right) \\
&= \delta(\rho).
\end{aligned} \tag{40}$$

Combining Equation (40) and (37), we know that Equation (36) holds. This leads to

$$S_1 \xrightarrow{w} \max_{\rho \in [\rho_0, \rho_1]} \left(\frac{\sum_l \left(\sqrt{\lambda_l} W^0(\rho) + \xi(\rho) \Delta_l^{(1)} \right)^2 - \delta(\rho)}{\rho(1-\rho)} \right).$$

□

B.4.2 Proof of Theorem B.2

Proof. Define $\tilde{\epsilon}_i = z_i - \mu_{t-}$ for all $i = 1, 2, \dots, t$ and $\tilde{\epsilon}_i = z_i - \mu_{t+}$ for all $i = t + 1, \dots, n$.

Notice that

$$\begin{aligned} \frac{1}{\sqrt{n}\widehat{s}_n} \frac{t(n-t)}{2n} (\bar{d}_{B_1(t)} - \bar{d}_{B_2(t)}) &= \frac{1}{\sqrt{n}} \frac{s}{\widehat{s}_n} \frac{1}{s} \left[\frac{t}{t-1} \frac{n-t}{n} \sum_{i=1}^t \|\tilde{\epsilon}_i\|^2 - \frac{n-t}{n-t-1} \frac{t}{n} \sum_{i=t+1}^n \|\tilde{\epsilon}_i\|^2 \right] \\ &+ \frac{1}{\widehat{s}_n} \frac{1}{\sqrt{n}} \frac{t}{t-1} \frac{n-t}{n} \sum_{i=1}^t (\|z_i - \bar{z}_t\|^2 - \|\tilde{\epsilon}_i\|^2) - \frac{1}{\widehat{s}_n} \frac{1}{\sqrt{n}} \frac{n-t}{n-t-1} \frac{t}{n} \sum_{i=t+1}^n (\|z_i - \bar{z}_{n-t}\|^2 - \|\tilde{\epsilon}_i\|^2) \\ &= U_1 + U_2 - U_3, \end{aligned}$$

where

$$\begin{aligned} U_1 &= \frac{1}{\sqrt{n}} \frac{s}{\widehat{s}_n} \frac{1}{s} \left[\frac{t}{t-1} \frac{n-t}{n} \sum_{i=1}^t \|\tilde{\epsilon}_i\|^2 - \frac{n-t}{n-t-1} \frac{t}{n} \sum_{i=t+1}^n \|\tilde{\epsilon}_i\|^2 \right], \\ U_2 &= \frac{1}{\widehat{s}_n} \frac{1}{\sqrt{n}} \frac{t}{t-1} \frac{n-t}{n} \sum_{i=1}^t (\|z_i - \bar{z}_t\|^2 - \|\tilde{\epsilon}_i\|^2), \quad U_3 = \frac{1}{\widehat{s}_n} \frac{1}{\sqrt{n}} \frac{n-t}{n-t-1} \frac{t}{n} \sum_{i=t+1}^n (\|z_i - \bar{z}_{n-t}\|^2 - \|\tilde{\epsilon}_i\|^2). \end{aligned}$$

Now we bound U_1, U_2, U_3 separately.

For U_1 , we have

$$\begin{aligned} U_1 &= \frac{1}{\sqrt{n}} \frac{s}{\widehat{s}_n} \frac{1}{s} \left[\frac{t}{t-1} \frac{n-t}{n} \sum_{i=1}^t (\|\tilde{\epsilon}_i\|^2 - \mathbb{E}\|\tilde{\epsilon}_i\|^2) - \frac{n-t}{n-t-1} \frac{t}{n} \sum_{i=t+1}^n (\|\tilde{\epsilon}_i\|^2 - \mathbb{E}\|\tilde{\epsilon}_i\|^2) \right] \\ &+ \frac{1}{\sqrt{n}\widehat{s}_n} \tau^*(1-\rho) \left(v_0 - v_1 + \frac{\rho - \rho^*}{\rho} \|\mu_0 - \mu_1\|^2 \right) \mathbf{1}(\rho \geq \rho^*) \\ &+ \frac{1}{\sqrt{n}\widehat{s}_n} (n - \tau^*) \rho \left(v_0 - v_1 - \frac{\rho^* - \rho}{1-\rho} \|\mu_0 - \mu_1\|^2 \right) \mathbf{1}(\rho < \rho^*). \end{aligned}$$

Since d is bounded, and $\widehat{s}_n \xrightarrow{p} s$ from Lemma B.5, we know

$$\frac{1}{\sqrt{n}} \frac{s}{\widehat{s}_n} \frac{1}{s} \left[\frac{t}{t-1} \frac{n-t}{n} \sum_{i=1}^t (\|\tilde{\epsilon}_i\|^2 - \mathbb{E}\|\tilde{\epsilon}_i\|^2) - \frac{n-t}{n-t-1} \frac{t}{n} \sum_{i=t+1}^n (\|\tilde{\epsilon}_i\|^2 - \mathbb{E}\|\tilde{\epsilon}_i\|^2) \right] \xrightarrow{w} G,$$

where G is some Gaussian process. Thus,

$$U_2 \xrightarrow{w} G + \Delta^{(2)}. \quad (41)$$

For U_2 , we have

$$\begin{aligned}
U_2 &= \frac{1}{\widehat{s}_n} \frac{1}{\sqrt{n}} \frac{t}{t-1} \frac{n-t}{n} \sum_{i=1}^t (\|z_i - \bar{z}_t\|^2 - \|\tilde{\epsilon}_i\|^2) \\
&= \frac{1}{\widehat{s}_n} \frac{1}{\sqrt{n}} \frac{t}{t-1} \frac{n-t}{n} \sum_{i=1}^t (\|z_i - \bar{\mu}_t - \bar{\epsilon}_t\|^2 - \|z_i - \bar{\mu}_t\|^2) \\
&= \frac{1}{\widehat{s}_n} \frac{1}{\sqrt{n}} \frac{t^2}{t-1} \frac{n-t}{n} (-\|\bar{\epsilon}_t\|^2) \xrightarrow{p} 0,
\end{aligned} \tag{42}$$

because $\|\bar{\epsilon}_t\| = \mathcal{O}_p(t^{-1/2})$ from Lemma B.1. Similarly we have

$$U_3 \xrightarrow{p} 0. \tag{43}$$

Combining Equation (41), (42), (43), we get

$$S_2 \xrightarrow{w} \max_{\rho \in [\rho_0, \rho_1]} \left(\frac{|G + \Delta^{(2)}|}{\sqrt{\rho(1-\rho)}} \right).$$

□

B.5 Proof of Theorem 4.3

B.5.1 For S_1

Proof. We will utilize the following equation: $\forall t \in \{1, 2, \dots, n\}$,

$$\begin{aligned}
T_1(t) &= \frac{1}{t} \sum_{i=1}^t \tilde{k}(y_i, y_i) + \frac{1}{n-t} \sum_{i=t+1}^n \tilde{k}(y_i, y_i) - 2\langle \bar{\phi}(y)_{t-}, \bar{\phi}(y)_{t+} \rangle \\
&\quad - \frac{1}{t-1} (\|(\boldsymbol{\mu}^*)_{t-} - (\boldsymbol{\mu})_{t-}\|^2 + 2\langle (\boldsymbol{\mu}^*)_{t-} - (\boldsymbol{\mu})_{t-}, (\boldsymbol{\epsilon})_{t-} \rangle - \|\Pi(\boldsymbol{\epsilon})_{t-}\|^2 + \|(\boldsymbol{\epsilon})_{t-}\|^2) \\
&\quad - \frac{1}{n-t-1} (\|(\boldsymbol{\mu}^*)_{t+} - (\boldsymbol{\mu})_{t+}\|^2 + 2\langle (\boldsymbol{\mu}^*)_{t+} - (\boldsymbol{\mu})_{t+}, (\boldsymbol{\epsilon})_{t+} \rangle - \|\Pi(\boldsymbol{\epsilon})_{t+}\|^2 + \|(\boldsymbol{\epsilon})_{t+}\|^2).
\end{aligned}$$

Suppose $\tau^* < \hat{\tau}$. Plugging the above equation into the basic inequality $S_1(\hat{\tau}) \geq S_1(\tau^*)$, we have

$$0 \leq \frac{\tau^* - \hat{\tau}}{n^2} \sum_{i=1}^{\tau^*} \tilde{k}(y_i, y_i) + \frac{n - \hat{\tau} - \tau^*}{n^2} \sum_{i=\tau^*+1}^{\hat{\tau}} \tilde{k}(y_i, y_i) + \frac{\hat{\tau} - \tau^*}{n^2} \sum_{i=\hat{\tau}+1}^n \tilde{k}(y_i, y_i) \quad (44)$$

$$+ \frac{\tau^* - \hat{\tau}}{n^2} \sum_{i=1}^{\tau^*} \|\epsilon_i\|^2 + \frac{n - \hat{\tau} - \tau^*}{n^2} \sum_{i=\tau^*+1}^{\hat{\tau}} \|\epsilon_i\|^2 + \frac{\hat{\tau} - \tau^*}{n^2} \sum_{i=\hat{\tau}+1}^n \|\epsilon_i\|^2 \quad (45)$$

$$- \frac{\hat{\tau}(n - \hat{\tau})}{n^2(\hat{\tau} - 1)} \|(\boldsymbol{\mu}^*)_{\hat{\tau}-} - (\boldsymbol{\mu})_{\hat{\tau}-}\|^2 - \frac{\hat{t}(n - \hat{t})}{n^2(n - \hat{t} - 1)} \|(\boldsymbol{\mu}^*)_{\hat{\tau}+} - (\boldsymbol{\mu})_{\hat{\tau}+}\|^2 \quad (46)$$

$$- \frac{2\hat{\tau}(n - \hat{\tau})}{n^2(\hat{\tau} - 1)} \langle (\boldsymbol{\mu}^*)_{\hat{\tau}-} - (\boldsymbol{\mu})_{\hat{\tau}-}, (\boldsymbol{\epsilon})_{\tau^*-} \rangle - \frac{2\hat{\tau}(n - \hat{\tau})}{n^2(n - \hat{\tau} - 1)} \langle (\boldsymbol{\mu}^*)_{\hat{\tau}+} - (\boldsymbol{\mu})_{\hat{\tau}+}, (\boldsymbol{\epsilon})_{\tau^*+} \rangle \quad (47)$$

$$+ \frac{\hat{\tau}(n - \hat{\tau})}{n^2(\hat{\tau} - 1)} \|\Pi(\boldsymbol{\epsilon})_{\hat{\tau}-}\|^2 + \frac{\hat{\tau}(n - \hat{\tau})}{n^2(n - \hat{\tau} - 1)} \|\Pi(\boldsymbol{\epsilon})_{\hat{\tau}+}\|^2 \quad (48)$$

$$- \frac{\tau^*(n - \tau^*)}{n^2(\tau^* - 1)} \|\Pi(\boldsymbol{\epsilon})_{\tau^*-}\|^2 - \frac{\tau^*(n - \tau^*)}{n^2(n - \tau^* - 1)} \|\Pi(\boldsymbol{\epsilon})_{\tau^*+}\|^2 \quad (49)$$

$$- \frac{2\hat{\tau}(n - \hat{\tau})}{n^2} \langle \bar{\phi}(y)_{\hat{\tau}-}, \bar{\phi}(y)_{\hat{\tau}+} \rangle + \frac{2\tau^*(n - \tau^*)}{n^2} \langle \bar{\phi}(y)_{\tau^*-}, \bar{\phi}(y)_{\tau^*+} \rangle. \quad (50)$$

Now we will bound each line separately.

Define $U_1 = \frac{\tau^* - \hat{\tau}}{n^2} \tau^* \|\mu_0\|^2 + \frac{(\hat{\tau} - \tau^*)(2n - 2\hat{\tau} - \tau^*)}{n^2} \|\mu_1\|^2$. Then for line (44) and line (45), we have for any $x > 0$,

$$\begin{aligned} & (44) + (45) \\ &= \frac{\tau^* - \hat{\tau}}{n^2} \sum_{i=1}^{\tau^*} (\|\mu_0\|^2 + 2\langle \mu_0, \epsilon_i \rangle) + \frac{n - \hat{\tau} - \tau^*}{n^2} \sum_{i=\tau^*+1}^{\hat{\tau}} (\|\mu_1\|^2 + 2\langle \mu_1, \epsilon_i \rangle) + \frac{\hat{\tau} - \tau^*}{n^2} (\|\mu_1\|^2 + 2\langle \mu_1, \epsilon_i \rangle) \\ &= \frac{\tau^* - \hat{\tau}}{n^2} \tau^* \|\mu_0\|^2 + \frac{(\hat{\tau} - \tau^*)(2n - 2\hat{\tau} - \tau^*)}{n^2} \|\mu_1\|^2 \\ & \quad + 2 \frac{\tau^* - \hat{\tau}}{n^2} \sum_{i=1}^{\tau^*} \langle \mu_0, \epsilon_i \rangle + 2 \frac{n - \hat{\tau} - \tau^*}{n^2} \sum_{i=\tau^*+1}^{\hat{\tau}} \langle \mu_1, \epsilon_i \rangle + 2 \frac{\hat{\tau} - \tau^*}{n^2} \sum_{i=\hat{\tau}+1}^n \langle \mu_1, \epsilon_i \rangle, \end{aligned}$$

where from Cauchy-Schwarz Inequality, Lemma B.1 and the fact that $\|\mu^i\|^2 \leq \mathbb{E}_{F^i} \|\phi(y)\|^2 =$

$\mathbb{E}_{F^i} \tilde{k}(y, y) \leq M^2$, we know

$$\begin{aligned} \frac{\tau^* - \hat{\tau}}{n^2} \sum_{i=1}^{\tau^*} \langle \mu_0, \epsilon_i \rangle &\leq \frac{|\tau^* - \hat{\tau}|}{n^2} \|\mu_0\| \left\| \sum_{i=1}^{\tau^*} \epsilon_i \right\| \leq \frac{|\tau^* - \hat{\tau}|}{n^2} \sqrt{\frac{14\tau^*}{3}} (\sqrt{x} + \sqrt{2}) M^2, \quad \text{w.p. at least } 1 - 2e^{-x}. \\ \frac{n - \hat{\tau} - \tau^*}{n^2} \sum_{i=\tau^*+1}^{\hat{\tau}} \langle \mu_1, \epsilon_i \rangle &\leq \frac{|n - \tau^* - \hat{\tau}|}{n^2} \sqrt{\frac{14(\hat{\tau} - \tau^*)}{3}} (\sqrt{x} + \sqrt{2}) M^2, \quad \text{w.p. at least } 1 - 2e^{-x}. \\ \frac{\hat{\tau} - \tau^*}{n^2} \sum_{i=\hat{\tau}+1}^n \langle \mu_1, \epsilon_i \rangle &\leq \frac{|\hat{\tau} - \tau^*|}{n^2} \sqrt{\frac{14(n - \hat{\tau})}{3}} (\sqrt{x} + \sqrt{2}) M^2, \quad \text{w.p. at least } 1 - 2e^{-x}. \end{aligned}$$

Thus, with probability at least $1 - 6e^{-x}$, we have

$$(44) + (45) \leq U_1 + 6M^2(\sqrt{x} + \sqrt{2}) \frac{1}{\sqrt{n}} \sqrt{\frac{\hat{\tau} - \tau^*}{n}}. \quad (51)$$

For line (46) and line (47), from Proposition 3 of Arlot et al. (2012), we have for any $\theta > 0$ and $x > 0$, with probability at least $1 - 4e^{-x}$,

$$\begin{aligned} (47) &\leq \frac{2\hat{\tau}(n - \hat{\tau})}{n^2(\hat{\tau} - 1)} \left[\theta \|(\boldsymbol{\mu}^*)_{\hat{\tau}-} - (\boldsymbol{\mu})_{\hat{\tau}-}\|^2 + \left(\frac{3v_0}{2} + \frac{4M^2}{3} \right) x \right] \\ &\quad + \frac{2\hat{\tau}(n - \hat{\tau})}{n^2(\hat{\tau} - 1)} \left[\theta \|(\boldsymbol{\mu}^*)_{\hat{\tau}+} - (\boldsymbol{\mu})_{\hat{\tau}+}\|^2 + \left(\frac{3v_1}{2} + \frac{4M^2}{3} \right) x \right]. \end{aligned}$$

Take $\theta = \frac{1}{3}$, we have with probability at least $1 - 4e^{-x}$,

$$(46) + (47) \stackrel{(a)}{\leq} -\frac{1}{3} \frac{\hat{\tau}(n - \hat{\tau})}{n^2(\hat{\tau} - 1)} (\hat{\tau} - \tau^*) \|\mu_0 - \mu_1\|^2 + \frac{17}{2n} M^2 x, \quad (52)$$

where (a) follows from the fact that $v_0 = \mathbb{E}_{F^i} \|\epsilon\|^2 \leq \mathbb{E}_{F^i} \|\mu^i + \epsilon_i\|^2 = \mathbb{E}_{F^i} \tilde{k}(y, y) \leq M^2$.

For line (48) and line (49), from Lemma B.1, we know that for any $x > 0$, with probability at least $1 - 2e^{-x}$, we have

$$(48) + (49) \leq \left(\frac{\hat{\tau}(n - \hat{\tau})}{n^2(\hat{\tau} - 1)} + \frac{\hat{\tau}(n - \hat{\tau})}{n^2(n - \hat{\tau} - 1)} \right) \left(M^2 + \frac{14}{3} M^2 (x + 2\sqrt{2x}) \right) \leq \frac{1}{n} \frac{28}{3} M^2 (\sqrt{x} + \sqrt{2})^2. \quad (53)$$

For line (50), we have

$$\begin{aligned} & -\frac{2\hat{\tau}(n - \hat{\tau})}{n^2} \langle \bar{\phi}(y)_{\hat{\tau}-}, \bar{\phi}(y)_{\hat{\tau}+} \rangle = -\frac{2}{n^2} \left\langle \tau^* \mu_0 + (\hat{\tau} - \tau^*) \mu_1 + \sum_{i=1}^{\hat{\tau}} \epsilon_i, (n - \hat{\tau}) \mu_1 + \sum_{i=\hat{\tau}+1}^n \epsilon_i \right\rangle \\ & = -\frac{2}{n^2} \left[\tau^* (n - \hat{\tau}) \langle \mu_0, \mu_1 \rangle + (\hat{\tau} - \tau^*) (n - \hat{\tau}) \|\mu_1\|^2 + \left\langle \tau^* \mu_0 + (\hat{\tau} - \tau^*) \mu_1, \sum_{i=\hat{\tau}+1}^n \epsilon_i \right\rangle \right] \\ & \quad - \frac{2}{n^2} \left[\left\langle \sum_{i=1}^{\hat{\tau}} \epsilon_i, (n - \hat{\tau}) \mu_1 \right\rangle + \left\langle \sum_{i=1}^{\hat{\tau}} \epsilon_i, \sum_{i=\hat{\tau}+1}^n \epsilon_i \right\rangle \right], \end{aligned}$$

and

$$\begin{aligned} & \frac{2\tau^*(n-\tau^*)}{n^2} \langle \bar{\phi}(y)_{\tau^*-}, \bar{\phi}(y)_{\tau^*+} \rangle \\ &= \frac{2}{n^2} \left[\tau^*(n-\tau^*) \langle \mu_0, \mu_1 \rangle + \left\langle \tau^* \mu_0, \sum_{i=\tau^*+1}^n \epsilon_i \right\rangle + \left\langle \sum_{i=1}^{\tau^*} \epsilon_i, (n-\tau^*) \mu_1 \right\rangle + \left\langle \sum_{i=1}^{\tau^*} \epsilon_i, \sum_{i=\tau^*+1}^n \epsilon_i \right\rangle \right]. \end{aligned}$$

Thus,

$$\begin{aligned} (50) &= \frac{2}{n^2} \left[\tau^*(\hat{\tau}-\tau^*) \langle \mu_0, \mu_1 \rangle - (\hat{\tau}-\tau^*)(n-\hat{\tau}) \|\mu_1\|^2 + \left\langle \sum_{i=1}^{\tau^*} \epsilon_i, (\hat{\tau}-\tau^*) \mu_1 \right\rangle \right. \\ &\quad \left. + \left\langle \sum_{i=\tau^*+1}^{\hat{\tau}} \epsilon_i, \tau^* \mu_0 - (n-\hat{\tau}) \mu_1 \right\rangle \right] \\ &\quad + \frac{2}{n^2} \left[\left\langle \sum_{i=\hat{\tau}+1}^n \epsilon_i, -(\hat{\tau}-\tau^*) \mu_1 \right\rangle + \left\langle \sum_{i=1}^{\tau^*} \epsilon_i, \sum_{i=\tau^*+1}^n \epsilon_i \right\rangle - \left\langle \sum_{i=1}^{\hat{\tau}} \epsilon_i, \sum_{i=\hat{\tau}+1}^n \epsilon_i \right\rangle \right], \end{aligned}$$

where from Lemma B.1, the following holds: for any $x > 0$,

$$\frac{2}{n^2} \left\langle \sum_{i=1}^{\tau^*} \epsilon_i, (\hat{\tau}-\tau^*) \mu_1 \right\rangle \leq \frac{2}{n^2} (\hat{\tau}-\tau^*) \|\mu_1\| \left\| \sum_{i=1}^{\tau^*} \epsilon_i \right\| \leq \frac{2}{n^2} (\hat{\tau}-\tau^*) M^2 \sqrt{\frac{14\tau^*}{3}} (\sqrt{x} + \sqrt{2}),$$

w.p. at least $1 - 2e^{-x}$.

$$\frac{2}{n^2} \left\langle \sum_{i=\tau^*+1}^{\hat{\tau}} \epsilon_i, \tau^* \mu_0 - (n-\hat{\tau}) \mu_1 \right\rangle \leq \frac{2}{n^2} (\tau^* + n - \hat{\tau}) M^2 \sqrt{\frac{14(\hat{\tau}-\tau^*)}{3}} (\sqrt{x} + \sqrt{2}),$$

w.p. at least $1 - 2e^{-x}$.

$$\frac{2}{n^2} \left\langle \sum_{i=\hat{\tau}+1}^n \epsilon_i, -(\hat{\tau}-\tau^*) \mu_1 \right\rangle \leq \frac{2}{n^2} (\hat{\tau}-\tau^*) M^2 \sqrt{\frac{14(\hat{\tau}-\tau^*)}{3}} (\sqrt{x} + \sqrt{2}),$$

w.p. at least $1 - 2e^{-x}$.

$$\frac{2}{n^2} \left\langle \sum_{i=1}^{\tau^*} \epsilon_i, \sum_{i=\tau^*+1}^n \epsilon_i \right\rangle \leq \frac{28}{3} \frac{1}{n^2} M^2 \sqrt{(n-\tau^*)\tau^*} (\sqrt{x} + \sqrt{2})^2, \quad \text{w.p. at least } 1 - 2e^{-x}.$$

$$\frac{2}{n^2} \left\langle \sum_{i=1}^{\hat{\tau}} \epsilon_i, \sum_{i=\hat{\tau}+1}^n \epsilon_i \right\rangle \leq \frac{28}{3} \frac{1}{n^2} M^2 \sqrt{(n-\hat{\tau})\hat{\tau}} (\sqrt{x} + \sqrt{2})^2, \quad \text{w.p. at least } 1 - 2e^{-x}.$$

Thus, we have with probability at least $1 - 10e^{-x}$,

$$\begin{aligned}
(50) &\leq \frac{2}{n^2} \left[\tau^*(\hat{\tau} - \tau^*)\langle \mu_0, \mu_1 \rangle - (\hat{\tau} - \tau^*)(n - \hat{\tau})\|\mu_1\|^2 + (\hat{\tau} - \tau^*)\sqrt{\frac{14\tau^*}{3}}(\sqrt{x} + \sqrt{2})M^2 \right] \\
&\quad + \frac{2}{n^2} \left[(\tau^* + n - \hat{\tau})\sqrt{\frac{14(\hat{\tau} - \tau^*)}{3}}(\sqrt{x} + \sqrt{2})M^2 + (\hat{\tau} - \tau^*)\sqrt{\frac{14(\hat{\tau} - \tau^*)}{3}}(\sqrt{x} + \sqrt{2})M^2 \right] \\
&\quad + \frac{2}{n^2} \left[\frac{14}{3}\sqrt{\tau^*(n - \tau^*)}M^2(\sqrt{x} + \sqrt{2})^2 + \frac{14}{3}\sqrt{\hat{\tau}(n - \hat{\tau})}M^2(\sqrt{x} + \sqrt{2})^2 \right] \\
&\stackrel{(a)}{\leq} \frac{2}{n^2}\tau^*(\hat{\tau} - \tau^*)\langle \mu_0, \mu_1 \rangle - \frac{2}{n^2}(\hat{\tau} - \tau^*)(n - \hat{\tau})\|\mu_1\|^2 \\
&\quad + 6\sqrt{\frac{14}{3}}M^2(\sqrt{x} + \sqrt{2})\frac{1}{\sqrt{n}}\sqrt{\frac{\hat{\tau} - \tau^*}{n}} + \frac{56}{3}\frac{M^2(\sqrt{x} + \sqrt{2})^2}{n},
\end{aligned} \tag{54}$$

where (a) follows from the fact that $\frac{\hat{\tau} - \tau^*}{n} \leq \sqrt{\frac{\hat{\tau} - \tau^*}{n}}$.

Thus, combining (51), (52), (53) and (54), we have: with probability at least $1 - 22e^{-x}$,

$$\begin{aligned}
0 &\leq -\frac{1}{2}\frac{\hat{\tau} - \tau^*}{n}(1 - \rho_1 + \rho_0)\|\mu_0 - \mu_1\|^2 + \frac{1}{n}\left(\frac{17}{2}x + 28(\sqrt{x} + \sqrt{2})^2\right)M^2 \\
&\quad + 12\sqrt{\frac{14}{3}}M^2(\sqrt{x} + \sqrt{2})\frac{1}{\sqrt{n}}\sqrt{\frac{\hat{\tau} - \tau^*}{n}}.
\end{aligned}$$

The solution to the above inequality is that

$$\frac{\hat{\tau} - \tau^*}{n} \leq \frac{1}{n} \left(\frac{12\sqrt{14/3}M^2(\sqrt{x} + \sqrt{2})}{(1 - \rho_1 + \rho_0)\|\mu_0 - \mu_1\|^2} \right)^2 + \frac{2}{n} \frac{17x/2 + 28(\sqrt{x} + \sqrt{2})^2}{(1 - \rho_1 + \rho_0)\|\mu_0 - \mu_1\|^2} M^2.$$

When $\hat{\tau} < \tau^*$, we can prove a similar inequality. Thus for all $\hat{\tau}$, the desired conclusion holds. \square

B.5.2 For S_2

Proof. First notice that $\forall t \in \{1, 2, \dots, n\}$, under the assumption that $\mu_0 = \mu_1$, we have

$$\bar{d}_{B_1(t)} - \bar{d}_{B_2(t)} = \frac{2}{t-1} \left(-\|\Pi(\epsilon)_{t-}\|^2 + \|(\epsilon)_{t-}\|^2 \right) - \frac{2}{n-t-1} \left(-\|\Pi(\epsilon)_{t+}\|^2 + \|(\epsilon)_{t+}\|^2 \right).$$

Plug this into the basic inequality, $\mathcal{S}_2(\hat{\tau}) \geq \mathcal{S}_1(\tau^*)$, we have

LHS :=

$$\begin{aligned} & \sqrt{\frac{(n-\tau^*)\tau^*}{n^2}} \times \left| -\frac{1}{\tau^*(\tau^*-1)} \left\| \sum_{i=1}^{\tau^*} \epsilon_i \right\|^2 + \frac{1}{\tau^*-1} \sum_{i=1}^{\tau^*} \|\epsilon_i\|^2 + \frac{1}{(n-\tau^*)(n-\tau^*-1)} \left\| \sum_{i=\tau^*+1}^n \epsilon_i \right\|^2 - \frac{1}{n-\tau^*-1} \sum_{i=\tau^*+1}^n \|\epsilon_i\|^2 \right| \\ & \leq \sqrt{\frac{(n-\hat{\tau})\hat{\tau}}{n^2}} \times \left| -\frac{1}{\hat{\tau}(\hat{\tau}-1)} \left\| \sum_{i=1}^{\hat{\tau}} \epsilon_i \right\|^2 + \frac{1}{\hat{\tau}-1} \sum_{i=1}^{\hat{\tau}} \|\epsilon_i\|^2 + \frac{1}{(n-\hat{\tau})(n-\hat{\tau}-1)} \left\| \sum_{i=\hat{\tau}+1}^n \epsilon_i \right\|^2 - \frac{1}{n-\hat{\tau}-1} \sum_{i=\hat{\tau}+1}^n \|\epsilon_i\|^2 \right| := \text{RHS}. \end{aligned}$$

We will deal with LHS and RHS separately. Now suppose that $v_0 > v_1$. When $\hat{\tau} \leq \tau^*$, we have, for any $x > 0$, when n is sufficiently large, the term inside the absolute value for RHS is positive with probability at least $1 - e^{-x}$, i.e., with probability at least $1 - e^{-x}$,

$$-\frac{1}{\hat{\tau}(\hat{\tau}-1)} \left\| \sum_{i=1}^{\hat{\tau}} \epsilon_i \right\|^2 + \frac{1}{\hat{\tau}-1} \sum_{i=1}^{\hat{\tau}} \|\epsilon_i\|^2 + \frac{1}{(n-\hat{\tau})(n-\hat{\tau}-1)} \left\| \sum_{i=\hat{\tau}+1}^n \epsilon_i \right\|^2 - \frac{1}{n-\hat{\tau}-1} \sum_{i=\hat{\tau}+1}^n \|\epsilon_i\|^2 \geq 0,$$

because Lemma B.1 implies

$$\begin{aligned} & -\frac{1}{\hat{\tau}(\hat{\tau}-1)} \left\| \sum_{i=1}^{\hat{\tau}} \epsilon_i \right\|^2 + \frac{1}{\hat{\tau}-1} \sum_{i=1}^{\hat{\tau}} \|\epsilon_i\|^2 + \frac{1}{(n-\hat{\tau})(n-\hat{\tau}-1)} \left\| \sum_{i=\hat{\tau}+1}^n \epsilon_i \right\|^2 - \frac{1}{n-\hat{\tau}-1} \sum_{i=\hat{\tau}+1}^n \|\epsilon_i\|^2 \\ & = -\frac{1}{\hat{\tau}(\hat{\tau}-1)} \left\| \sum_{i=1}^{\hat{\tau}} \epsilon_i \right\|^2 + \frac{1}{(n-\hat{\tau})(n-\hat{\tau}-1)} \left\| \sum_{i=\hat{\tau}+1}^n \epsilon_i \right\|^2 \\ & + \frac{1}{\hat{\tau}-1} \sum_{i=1}^{\hat{\tau}} (\|\epsilon_i\|^2 - v_i) - \frac{1}{n-\hat{\tau}-1} \sum_{i=\hat{\tau}+1}^n (\|\epsilon_i\|^2 - v_i) + \frac{\hat{\tau}}{\hat{\tau}-1} (v_0 - v_1) + \frac{v_1}{n-\hat{\tau}-1} \\ & = \mathcal{O}_p(n^{-1/2}) + \frac{\hat{\tau}}{\hat{\tau}-1} (v_0 - v_1) + \frac{v_1}{n-\hat{\tau}-1}. \end{aligned}$$

and $v_0 - v_1, v_1 > 0$.

Thus, for any $x > 0$, when n is sufficiently large, with probability at least $1 - e^{-x}$, we have

$$\begin{aligned} \text{RHS} & = \sqrt{\frac{(n-\hat{\tau})\hat{\tau}}{n^2}} \times \left(-\frac{1}{\hat{\tau}(\hat{\tau}-1)} \left\| \sum_{i=1}^{\hat{\tau}} \epsilon_i \right\|^2 + \frac{1}{(n-\hat{\tau})(n-\hat{\tau}-1)} \left\| \sum_{i=\hat{\tau}+1}^n \epsilon_i \right\|^2 + \frac{1}{\hat{\tau}-1} \sum_{i=1}^{\hat{\tau}} (\|\epsilon_i\|^2 - v_i) \right) \\ & + \sqrt{\frac{(n-\hat{\tau})\hat{\tau}}{n^2}} \times \left(-\frac{1}{n-\hat{\tau}-1} \sum_{i=\hat{\tau}+1}^n (\|\epsilon_i\|^2 - v_i) + \frac{t^*}{\hat{\tau}-1} (v_0 - v_1) + \frac{v_1}{n-\hat{\tau}-1} \right), \end{aligned}$$

and consequently from Lemma B.1, we know that with probability at least $1 - 5e^{-x}$,

$$\begin{aligned}
\text{RHS} &\leq \sqrt{\frac{(n - \hat{\tau})\hat{\tau}}{n^2}} \times \left(\frac{1}{(\hat{\tau} - 1)} \frac{14}{3} (\sqrt{x} + \sqrt{2})^2 M^2 + \frac{1}{(n - \hat{\tau} - 1)} \frac{14}{3} (\sqrt{x} + \sqrt{2})^2 M^2 \right. \\
&\quad \left. + \frac{1}{\hat{\tau} - 1} \sum_{i=1}^{\hat{\tau}} (\|\epsilon_i\|^2 - v_i) \right) \\
&\quad + \sqrt{\frac{(n - \hat{\tau})\hat{\tau}}{n^2}} \times \left(-\frac{1}{n - \hat{\tau} - 1} \sum_{i=\hat{\tau}+1}^n (\|\epsilon_i\|^2 - v_i) + \frac{\tau^*}{\hat{\tau} - 1} (v_0 - v_1) + \frac{v_1}{n - \hat{\tau} - 1} \right),
\end{aligned} \tag{55}$$

Similarly, for any $x > 0$, when n is sufficiently large, with probability at least $1 - 5e^{-x}$, we have

$$\begin{aligned}
\text{LHS} &= \sqrt{\frac{(n - \tau^*)\tau^*}{n^2}} \times \left| -\frac{1}{\tau^*(\tau^* - 1)} \left\| \sum_{i=1}^{\tau^*} \epsilon_i \right\|^2 + \frac{1}{(n - \tau^*)(n - \tau^* - 1)} \left\| \sum_{i=\tau^*+1}^n \epsilon_i \right\|^2 \right. \\
&\quad \left. + \frac{1}{\tau^* - 1} \sum_{i=1}^{\tau^*} (\|\epsilon_i\|^2 - v_i) - \frac{1}{n - \tau^* - 1} \sum_{i=\tau^*+1}^n (\|\epsilon_i\|^2 - v_i) + \frac{\tau^*}{\tau^* - 1} v_0 - \frac{(n - \tau^*)}{n - \tau^* - 1} v_1 \right| \\
&\geq \sqrt{\frac{(n - \tau^*)\tau^*}{n^2}} \times \left(-\frac{1}{(\tau^* - 1)} \frac{14}{3} (\sqrt{x} + \sqrt{2})^2 M^2 - \frac{1}{(n - \tau^* - 1)} \frac{14}{3} (\sqrt{x} + \sqrt{2})^2 M^2 \right. \\
&\quad \left. - \frac{1}{\tau^* - 1} \sum_{i=1}^{\tau^*} (\|\epsilon_i\|^2 - v_i) \right) \\
&\quad + \sqrt{\frac{(n - \tau^*)\tau^*}{n^2}} \times \left(-\frac{1}{n - \tau^* - 1} \sum_{i=\tau^*+1}^n (\|\epsilon_i\|^2 - v_i) + (v_0 - v_1) - \frac{v_1}{n - \tau^* - 1} \right. \\
&\quad \left. - \frac{v_0}{\tau^* - 1} \right),
\end{aligned} \tag{56}$$

Combing Equation (55) and Equation (56), for any $x > 0$, when n is sufficiently large, with

probability at least $1 - 10e^{-x}$, we have:

$$\begin{aligned}
& \left(\sqrt{\frac{(n - \tau^*)\tau^*}{n^2}} - \sqrt{\frac{(n - \hat{\tau})\hat{\tau}}{n^2} \frac{\tau^*}{\hat{\tau}}} \right) |v_0 - v_1| \\
\leq & \sqrt{\frac{(n - \hat{\tau})\hat{\tau}}{n^2}} \left[\frac{1}{n - \hat{\tau} - 1} v_1 + \frac{14}{3} \left(\frac{1}{n_0} + \frac{1}{n - n_1} \right) (\sqrt{x} + \sqrt{2})^2 M^2 \right] \\
& + \sqrt{\frac{(n - \tau^*)\tau^*}{n^2}} \left[\frac{1}{n - \tau^* - 1} v_1 + \frac{1}{\tau^* - 1} v_0 + \frac{14}{3} \left(\frac{1}{n_0} + \frac{1}{n - n_1} \right) (\sqrt{x} + \sqrt{2})^2 M^2 \right] \\
& + \sqrt{\frac{(n - \hat{\tau})\hat{\tau}}{n^2}} \left[\frac{\tau^*}{\hat{\tau} - 1} - \frac{\tau^*}{\hat{\tau}} \right] |v_0 - v_1| + \left(\sqrt{\frac{(n - \hat{\tau})\hat{\tau}}{n^2} \frac{1}{\hat{\tau} - 1}} - \sqrt{\frac{(n - \tau^*)\tau^*}{n^2} \frac{1}{\tau^* - 1}} \right) \sum_{i=1}^{\tau^*} (\|\epsilon_i\|^2 - v_i) \\
& + \left(\sqrt{\frac{(n - \hat{\tau})\hat{\tau}}{n^2} \frac{1}{\hat{\tau} - 1}} + \sqrt{\frac{(n - \tau^*)\tau^*}{n^2} \frac{1}{n - \tau^* - 1}} \right) \sum_{i=\tau^*+1}^{\hat{\tau}} (\|\epsilon_i\|^2 - v_i) \\
& - \left(\sqrt{\frac{(n - \hat{\tau})\hat{\tau}}{n^2} \frac{1}{n - \hat{\tau} - 1}} - \sqrt{\frac{(n - \tau^*)\tau^*}{n^2} \frac{1}{n - \tau^* - 1}} \right) \sum_{i=\hat{\tau}+1}^n (\|\epsilon_i\|^2 - v_i).
\end{aligned}$$

Utilizing Proposition 4 in [Arlot et al. \(2012\)](#) and the fact that $0 < v_0, v_1 \leq M^2$, for any

$x > 0$, when n is sufficiently large, with probability at least $1 - 16e^{-x}$, we have:

$$\begin{aligned}
& \left(\sqrt{\frac{(n - \tau^*)\tau^*}{n^2}} - \sqrt{\frac{(n - \widehat{\tau})\widehat{\tau}\tau^*}{n^2}} \right) |v_0 - v_1| \\
& \leq \frac{1}{2} \left[\frac{2}{n - n_1} M^2 + \frac{2}{n_0} M^2 + \frac{28}{3} \left(\frac{1}{n_0} + \frac{1}{n - n_1} \right) (\sqrt{x} + \sqrt{2})^2 M^2 \right] \\
& \quad + \frac{2}{n} \left(\sqrt{\frac{n - \widehat{\tau}}{\widehat{\tau}}} - \sqrt{\frac{n - \tau^*}{\tau^*}} \right) \left(\sqrt{2\tau^* M^4 x} + \frac{M^2}{3} x \right) \\
& \quad + \frac{2}{n} \left(\sqrt{\frac{n - \widehat{\tau}}{\widehat{\tau}}} + \sqrt{\frac{\tau^*}{n - \tau^*}} \right) \left(\sqrt{2(\widehat{\tau} - \tau^*) M^4 x} + \frac{M^2}{3} x \right) \\
& \quad + \frac{2}{n} \left(\sqrt{\frac{\widehat{\tau}}{n - \widehat{\tau}}} - \sqrt{\frac{\tau^*}{n - \tau^*}} \right) \left(\sqrt{2(n - \widehat{\tau}) M^4 x} + \frac{M^2}{3} x \right) \\
& \leq \frac{1}{2} \left[\frac{2}{n - n_1} M^2 + \frac{2}{n_0} M^2 + \frac{28}{3} \left(\frac{1}{n_0} + \frac{1}{n - n_1} \right) (\sqrt{x} + \sqrt{2})^2 M^2 \right] \\
& \quad + \frac{2}{n} \left(2\sqrt{\frac{n - \widehat{\tau}}{\widehat{\tau}}} - \sqrt{\frac{n - \tau^*}{\tau^*}} + \sqrt{\frac{\widehat{\tau}}{n - \widehat{\tau}}} \right) \frac{M^2}{3} x \\
& \quad + \frac{2}{n} \left(\sqrt{\frac{n - \tau^*}{n - \widehat{\tau}}} - \sqrt{\frac{\tau^*}{\widehat{\tau}}} \right) \sqrt{n - \widehat{\tau}} \left(\sqrt{\frac{\widehat{\tau}}{n - \tau^*}} - 1 \right) \sqrt{2M^4 x} \\
& \quad + \frac{2}{n} \left(\sqrt{\frac{n - \widehat{\tau}}{\widehat{\tau}}} + \sqrt{\frac{\tau^*}{n - \tau^*}} \right) \sqrt{\frac{\widehat{\tau} - \tau^*}{n}} \sqrt{2M^4 x}.
\end{aligned}$$

Let

$$\begin{aligned}
c_1 &= \frac{1}{2} \left[\frac{2}{n - n_1} M^2 + \frac{2}{n_0} M^2 + \frac{28}{3} \left(\frac{1}{n_0} + \frac{1}{n - n_1} \right) (\sqrt{x} + \sqrt{2})^2 M^2 \right] \\
& \quad + \frac{2}{n} \left(2\sqrt{\frac{n - \widehat{\tau}}{\widehat{\tau}}} - \sqrt{\frac{n - \tau^*}{\tau^*}} + \sqrt{\frac{\widehat{\tau}}{n - \widehat{\tau}}} \right) \frac{M^2}{3} x, \\
c_2 &= \sqrt{\frac{\tau^*(n - \widehat{\tau})}{n^2}} (v_0 - v_1) - \frac{2}{n} \sqrt{n - \widehat{\tau}} \left(\sqrt{\frac{\widehat{\tau}}{n - \tau^*}} - 1 \right) \sqrt{2M^4 x}, \\
w &= \frac{\widehat{\tau} - \tau^*}{n}, \quad c_3 = \frac{2}{\sqrt{n}} \left(\sqrt{\frac{n - \widehat{\tau}}{\widehat{\tau}}} + \sqrt{\frac{\tau^*}{n - \tau^*}} \right) \sqrt{2M^4 x}.
\end{aligned}$$

Then, we have: for any $x > 0$, when n is sufficiently large, with probability at least $1 - 16e^{-x}$,

$$c_2 \left(\sqrt{1 + \frac{w}{1 - w - \rho^*}} - \sqrt{1 - \frac{w}{w + \rho^*}} \right) \leq c_1 + c_3 \sqrt{w}.$$

Using the fact that

$$c_2 \left(\sqrt{1 + \frac{w}{1 - w - \rho^*}} - \sqrt{1 - \frac{w}{w + \rho^*}} \right) \geq c_2 \left(\sqrt{1 + w} - 1 \right) \stackrel{(a)}{\geq} c_2(\sqrt{2} - 1)w,$$

where (a) follows from the fact that $\sqrt{1 + w} \geq 1 + (\sqrt{2} - 1)w$ for any $w > 0$. We have for any $x > 0$, when n is sufficiently large, with probability at least $1 - 16e^{-x}$,

$$c_2(\sqrt{2} - 1)w \leq c_1 + c_3\sqrt{w}. \quad (57)$$

Notice that

$$\begin{aligned} c_1 &\leq \frac{1}{n} \left[\frac{1}{1 - \rho_1} M^2 + \frac{1}{\rho_0} M^2 + \frac{14}{3} \left(\frac{1}{\rho_0} + \frac{1}{1 - \rho_1} \right) (\sqrt{x} + \sqrt{2})^2 M^2 \right] + \frac{2}{n} \left(2\sqrt{\frac{1 - \rho_0}{\rho_0}} + \sqrt{\frac{\rho_1}{1 - \rho_1}} \right) \frac{M^2}{3} x, \\ c_2 &\geq \sqrt{\rho^*(1 - \rho_1)}(v_0 - v_1) - \frac{2}{\sqrt{n}} \sqrt{1 - \rho_0} \left(\sqrt{\frac{\rho_1}{1 - \rho^*}} - 1 \right) \sqrt{2M^4 x}, \\ c_3 &\leq \frac{2}{\sqrt{n}} \left(\sqrt{\frac{1 - \rho_0}{\rho_0}} + \sqrt{\frac{\rho^*}{1 - \rho^*}} \right) \sqrt{2M^4 x}. \end{aligned}$$

Thus, $c_2 > c_3\sqrt{\rho^*(1 - \rho_1)}(v_0 - v_1)$ when n is sufficiently large.

So Equation (57) yields: for any $x > 0$, when n is sufficiently large, with probability at least $1 - 16e^{-x}$,

$$\begin{aligned} w &\leq \left(\frac{c_3}{2c_2(\sqrt{2} - 1)} + \sqrt{\frac{c_1}{c_2(\sqrt{2} - 1)} + \frac{c_3^2}{4c_2^2(\sqrt{2} - 1)^2}} \right)^2 \stackrel{(b)}{\leq} \frac{c_3^2}{c_2^2(\sqrt{2} - 1)^2} + \frac{2c_1}{c_2(\sqrt{2} - 1)} \\ &\leq \tilde{C}_0 \frac{1}{n} \left(\frac{M^4 x}{(v_0 - v_1)^2} + \frac{M^2 x}{|v_0 - v_1|} \right), \end{aligned}$$

where (b) utilizes the fact that $(x + y)^2 \leq 2(x^2 + y^2)$ for all x, y . \square

B.6 Derivation for Higher Order Correction for S_2 (Equation

(20), (22))

First we derive Equation (20): From Proof of Lemma B.4, we know that

$$\frac{\sqrt{n}\rho(1 - \rho)}{2\widehat{s}_n} T_2 = U_1 + U_2 + U_3,$$

where

$$\begin{aligned}
U_1 &= \frac{1}{\sqrt{ns_n}} \left[\frac{t}{t-1} \frac{n-t}{n} \sum_{i=1}^t \|\epsilon_i\|^2 - \frac{n-t}{n-t-1} \frac{t}{n} \sum_{i=t+1}^n \|\epsilon_i\|^2 \right] \xrightarrow{w} W^0(\rho), \\
U_2 &= -\frac{1}{\sqrt{n\widehat{s}_n}} \frac{t}{t-1} \left(1 - \frac{t}{n}\right) \frac{1}{t} \sum_{i=1}^t \|\epsilon_i\|^2 \approx -\frac{1}{\sqrt{n\widehat{s}_n}} \frac{t}{t-1} \left(1 - \frac{t}{n}\right) \mathbb{E}\|\epsilon\|^2, \\
U_3 &= -\frac{1}{\sqrt{n\widehat{s}_n}} \frac{n-t}{n-t-1} \frac{t}{n} \frac{1}{n-t} \sum_{i=t+1}^n \|\epsilon_i\|^2 \approx -\frac{1}{\sqrt{n\widehat{s}_n}} \frac{n-t}{n-t-1} \frac{t}{n} \mathbb{E}\|\epsilon\|^2.
\end{aligned}$$

Thus, $U_2 = \mathcal{O}_p(n^{-1/2})$ and $U_3 = \mathcal{O}_p(n^{-1/2})$. By replacing the true mean with the estimated sample version, we can get Equation (20), which cancels the $\mathcal{O}_p(n^{-1/2})$ term from U_2 and U_3 .

Equation (22) corrects for the $\mathcal{O}_p(n^{-1/2})$ coming from U_1 : Write $Z\left(\frac{t}{n}\right) = \frac{U_1}{\sqrt{\rho(1-\rho)}}$. Following Chen et al. (2015), we have

$$\begin{aligned}
&\mathbb{P}\left(\max_{n_0 \leq t \leq n_1} Z\left(\frac{t}{n}\right) > b\right) \\
&= \frac{1}{b} \sum_{n_0 \leq t \leq n_1} \int_{x=0}^{\infty} p\left(Z\left(\frac{t}{n}\right) = b + \frac{1}{b}x\right) \mathbb{P}\left(\max_{n_0 \leq s \leq n_1} Z\left(\frac{s}{n}\right) < b \mid Z\left(\frac{t}{n}\right) = b + \frac{1}{b}x\right) dx.
\end{aligned}$$

We approximate $p\left(Z\left(\frac{t}{n}\right) = b + \frac{1}{b}x\right)$ using 3rd order Edgeworth Expansion and approximate $\mathbb{P}\left(\max_{n_0 \leq s \leq n_1} Z\left(\frac{s}{n}\right) < b \mid Z\left(\frac{t}{n}\right)\right)$ using a random walk.

Notice that $Z\left(\frac{t}{n}\right)$ is a sum of independent, non-identical distributed random variables, so we can apply Edgeworth Expansion and get when $b \rightarrow \infty$, $x^2/(2b^2)$ is negligible to x and x/b is negligible to b , so let V be the skewness of $Z\left(\frac{t}{n}\right)$, then

$$\begin{aligned}
&p\left(Z\left(\frac{t}{n}\right) = b + \frac{1}{b}x\right) \approx \phi\left(b + \frac{1}{b}x\right) + \frac{1}{\sqrt{n}} \frac{1}{6} V \left[\left(b + \frac{x}{b}\right)^3 - 3\left(b + \frac{x}{b}\right) \right] \phi\left(b + \frac{x}{b}\right) \\
&= \phi(b) e^{-x^2/(2b^2) - x} \left[1 + \frac{1}{6\sqrt{n}} V \left(b + \frac{x}{b}\right) \left(\left(b + \frac{x}{b}\right)^2 - 3 \right) \right] \\
&\approx \phi(b) e^{-x} \left[1 + \frac{1}{6\sqrt{n}} V b (b^2 - 3) \right].
\end{aligned}$$

To approximate $\mathbb{P}\left(\max_{n_0 \leq s \leq n_1} Z\left(\frac{s}{n}\right) < b \mid Z\left(\frac{t}{n}\right)\right)$, notice that

$$b\left(Z\left(\frac{s}{n}\right) - Z\left(\frac{t}{n}\right)\right) \mid Z\left(\frac{t}{n}\right) = b + \frac{x}{b} \sim N\left(-f'_{t/n,-}(0) \frac{s-t}{n} |b^2, 2f'_{t/n,-}(0) \frac{s-t}{n} |b^2\right),$$

where

$$f'_{x,-}(0) = \frac{\partial}{\partial \delta} \text{corr}(Z(0), Z(\delta)) \big|_{\delta=0} = \frac{1}{2x(1-x)}.$$

So let $W_m^{(t)}$ be a random walk with $W_1^{(t)} \sim N(\mu^{(t)}, (\sigma^2)^{(t)})$ where $\mu^{(t)} = \frac{1}{n} f_{t/n,-}(0) b^2$ and $(\sigma^2)^{(t)} = 2\mu^{(t)}$. We have

$$\mathbb{P} \left(\max_{n_0 \leq s \leq n_1} Z \left(\frac{s}{n} \right) < b \mid Z \left(\frac{t}{n} \right) \right) \approx \mathbb{P} \left(\max_{n_0 \leq s < t} -W_{t-s}^{(t)} < -x \right) \approx \mathbb{P} \left(\min_{m \geq 1} W_m^{(t)} > x \right).$$

Combining the above, we have

$$\begin{aligned} \mathbb{P} \left(\max_{n_0 \leq t \leq n_1} Z \left(\frac{t}{n} \right) > b \right) &\approx \frac{\phi(b)}{b} \left[1 + \frac{1}{6\sqrt{n}} V b (b^2 - 3) \right] \sum_{n_0 \leq t \leq n_1} \int_{x=0}^{\infty} e^{-x} \mathbb{P} \left(\min_{m \geq 1} W_m^{(t)} > x \right) dx \\ &= \frac{\phi(b)}{b} \left[1 + \frac{1}{6\sqrt{n}} V b (b^2 - 3) \right] \sum_{n_0 \leq t \leq n_1} (-f_{t/n,-}(0)) b^2 \nu \left(b \sqrt{-\frac{2}{n} f_{t/n,-}(0)} \right) \\ &= b \phi(b) \int_{\rho_1}^{\rho_1} \left[1 + \frac{1}{6\sqrt{n}} V b (b^2 - 3) \right] (-f_{x,-}(0)) \nu \left(b \sqrt{-2f_{x,-}(0)} \right) dx. \end{aligned}$$

And calculation shows (recall that $v = \mathbb{E} \|\epsilon\|^2$)

$$V = \frac{n-2t}{\sqrt{t(n-t)}} \times \text{Skewness of } \|\epsilon\|^2 = \frac{n-2t}{\sqrt{t(n-t)}} \times \frac{\mathbb{E} [\|\epsilon\|^6 - 3\|\epsilon\|^4 v + 3\|\epsilon\|^2 v^2 - v^3]}{[\mathbb{E} (\|\epsilon\|^4 - 2\|\epsilon\|^2 v + v^2)]^{1.5}}.$$

From symmetry of $Z \left(\frac{t}{n} \right)$, we know $\mathbb{P} \left(\max_{n_0 \leq t \leq n_1} |Z \left(\frac{t}{n} \right)| > b \right) = 2\mathbb{P} \left(\max_{n_0 \leq t \leq n_1} Z \left(\frac{t}{n} \right) > b \right)$.

By replacing the corresponding true moments by the sample version in K , we get Equation (22).

B.7 Proof of Proposition 2

Proof. First notice that

$$\lim_{n \rightarrow \infty} nT_1(t) = \lim_{n \rightarrow \infty} n \|\bar{\phi}(y)_{t-} - \bar{\phi}(y)_{t+}\|^2 + o_p(1).$$

And

$$\begin{aligned} \lim_{n \rightarrow \infty} \sqrt{n}T_2(t) &= \lim_{n \rightarrow \infty} \sqrt{n} \left[\frac{1}{t} \sum_{i=1}^t (\|\phi(y_i) - \bar{\phi}(y)_{t-}\|^2 - \mathbb{E} \|\phi(y_i) - \bar{\phi}(y)_{t-}\|^2) \right] \\ &\quad - \sqrt{n} \left[\frac{1}{n-t} \sum_{i=t+1}^n (\|\phi(y_i) - \bar{\phi}(y)_{t-}\|^2 - \mathbb{E} \|\phi(y_i) - \bar{\phi}(y)_{t-}\|^2) \right] + o_p(1). \end{aligned}$$

Notice that

$$\begin{aligned} & \sqrt{n} (\bar{\phi}_l(y)_{t-} - \mathbb{E}\bar{\phi}_l(y)_{t-}), \\ & \sqrt{n} (\bar{\phi}_l(y)_{t+} - \mathbb{E}\bar{\phi}_l(y)_{t+}), \\ & \frac{1}{\sqrt{n}} \sum_{i=1}^t [\|\phi(y_i) - \bar{\phi}(y)_{t-}\|^2 - \mathbb{E}\|\phi(y_i) - \bar{\phi}(y)_{t-}\|^2], \\ & \frac{1}{\sqrt{n}} \sum_{i=t+1}^n [\|\phi(y_i) - \bar{\phi}(y)_{t+}\|^2 - \mathbb{E}\|\phi(y_i) - \bar{\phi}(y)_{t+}\|^2], \end{aligned}$$

are all asymptotically Gaussian with mean 0. Thus, we only need to check that their covariance converges to 0. Since our data are i.i.d, we only need to check that the pairs:

$$\begin{aligned} & \sqrt{n} (\bar{\phi}_l(y)_{t-} - \mathbb{E}\bar{\phi}_l(y)_{t-}) \quad \text{and} \quad \frac{1}{\sqrt{n}} \sum_{i=1}^t \|\phi(y_i) - \bar{\phi}(y)_{t-}\|^2 - \mathbb{E}\|\phi(y_i) - \bar{\phi}(y)_{t-}\|^2, \\ & \sqrt{n} (\bar{\phi}_l(y)_{t+} - \mathbb{E}\bar{\phi}_l(y)_{t+}) \quad \text{and} \quad \frac{1}{\sqrt{n}} \sum_{i=t+1}^n \|\phi(y_i) - \bar{\phi}(y)_{t+}\|^2 - \mathbb{E}\|\phi(y_i) - \bar{\phi}(y)_{t+}\|^2, \end{aligned}$$

are asymptotically uncorrelated for any l . Since under the null,

$$\begin{aligned} & \text{Cov} \left(\sqrt{n} (\bar{\phi}_l(y)_{t-} - \mathbb{E}\bar{\phi}_l(y)_{t-}), \frac{1}{\sqrt{n}} \sum_{i=1}^t \|\phi(y_i) - \bar{\phi}(y)_{t-}\|^2 - \mathbb{E}\|\phi(y_i) - \bar{\phi}(y)_{t-}\|^2 \right) \\ & = \sum_{i=1}^t \mathbb{E}\|\phi(y_i) - \bar{\phi}(y)_{t-}\|^2 (\bar{\phi}_l(y)_t - \mathbb{E}\bar{\phi}_l(y)_{t-}) = \left(1 - \frac{1}{t}\right) \mathbb{E}\|\phi(y_i)\|^2 \phi_l(y_i) = 0. \end{aligned}$$

Similarly we have

$$\text{Cov} \left(\sqrt{n} (\bar{\phi}_l(y)_{t+} - \mathbb{E}\bar{\phi}_l(y)_{t+}), \frac{1}{\sqrt{n}} \sum_{i=t+1}^n \|\phi(y_i) - \bar{\phi}(y)_{t+}\|^2 - \mathbb{E}\|\phi(y_i) - \bar{\phi}(y)_{t+}\|^2 \right) = 0.$$

Thus, we get the desired conclusion. \square

B.8 Theoretical Guarantees for S_3

Corollary B.1 (Asymptotic null distribution for S_3). *Under H_0 , if distance d satisfies*

- (1) d is a semi-metric of negative type,
- (2) $\mathbb{E}_y |\tilde{k}(y, y)|^{2+\delta} + \mathbb{E}_{y, y'} |\tilde{k}(y, y')|^2 < +\infty$ for some $\delta > 0$,

(3) $\mathbb{E}_y |\tilde{k}(y, y) - \mathbb{E}\tilde{k}(y, y)|^{2+\delta} < +\infty$ for some $\delta' > 0$,

then as $n \rightarrow \infty$,

$$S_3 \xrightarrow{w} \max_{\rho_0 \leq \rho \leq \rho_1} \frac{1}{\rho(1-\rho)} (W^0(\rho))^2. \quad (58)$$

Proof. Corollary B.1 is a direct consequence of Theorem 4.1. \square

Corollary B.2 (Localization Consistency for S_3). *In AMOC setting, under H_A , suppose d is a semi-metric of negative type, and there exists some positive constant M such that for all $i \in \{1, \dots, n\}$, $\tilde{k}(y_i, y_i) \leq M^2$, a.s., then*

$$\left| \frac{\hat{\tau} - \tau^*}{n} \right| = o_p(1),$$

where $\hat{\tau}$ is the estimated change point using statistics S_3 .

Proof. From the proof of Theorem 4.2 (Section B.4), we know that

$$T_1 \xrightarrow{w} \frac{\|\mathbf{W}^0(\rho) + \xi(\rho)\mathbf{\Delta}^{(1)}\|^2 - \delta(\rho)}{n\rho^2(1-\rho)^2} = \left(\frac{\xi(\rho)}{\rho(1-\rho)} \right)^2 \|\mu_0 - \mu_1\|^2.$$

It is obvious that the maximum of $\left(\frac{\xi(\rho)}{\rho(1-\rho)} \right)^2$ is obtained at $\rho = \rho^*$. From the Argmax Theorem, we know that $\frac{\hat{\tau}}{n} - \frac{\tau^*}{n} = o_p(1)$. \square

Corollary B.3 (Power for S_3). *In AMOC setting, if (1) d is a semi-metric of negative type, (2) there exists some positive constant M such that for all $i \in \{1, \dots, n\}$, $\tilde{k}(y_i, y_i) \leq M^2$, a.s., then*

$$\mathbb{P}_{H_A} (S_3 > q_\alpha^{(2)}) \rightarrow 1, \quad n \rightarrow \infty,$$

if either $\sqrt{n}\|\mu_0 - \mu_1\|^2 \rightarrow \infty$ or $\sqrt{n}|v_0 - v_1| \rightarrow \infty$.

Proof. Corollary B.2 is a direct consequence of Theorem B.1 and Theorem B.2. \square

B.9 Proof of Theorem 4.4

Proof. For S_1 , using exactly the same techniques as in Theorem 4.1, it is easy to show that under the alternative, for all $t \in [l', r']$ where $l' = l + \lceil (r-l)\rho_0 \rceil$, $r' = l + \lceil (r-l)\rho_1 \rceil$, we have

$$T_1^{l,r}(t) \xrightarrow{p} \lim_{l,r \rightarrow \infty} \left\| \frac{1}{t-l} \sum_{i=l}^t \mathbb{E}_{F^i} \phi(y) \frac{1}{u-t} \sum_{i=t+1}^r \mathbb{E}_{F^i} \phi(y) \right\|^2 \quad \text{uniformly.}$$

This implies that under the alternative, as $n \rightarrow \infty$,

$$S_1^{l,r} = \max_{l' \leq t' \leq r'} \frac{(t-l)(r-t)}{r-l} T_1^{l,r}(t) \xrightarrow{p} \lim_{l,r \rightarrow \infty} \frac{(t-l)(r-t)}{r-l} \left\| \frac{1}{t-l} \sum_{i=l}^t \mathbb{E}_{F^i} \phi(y) \frac{1}{u-t} \sum_{i=t+1}^r \mathbb{E}_{F^i} \phi(y) \right\|^2 = \mathcal{O}(n).$$

Notice that

$$\mathbb{P}_{H_0}(S \geq s) \leq \alpha \quad \Leftrightarrow \quad s \geq q_\alpha,$$

where

$$q_\alpha = \text{upper } \alpha\text{-th quantile of } \max_{\rho_0 \leq \rho \leq \rho_1} \frac{\sum_{l=1}^{\infty} \lambda_l (W_l^0(\rho)^2 - \rho(1-\rho))}{\rho(1-\rho)}.$$

Thus, for S_1 , when $n \rightarrow \infty$, $\alpha \rightarrow 0$, $n\alpha \rightarrow \infty$, we have

$$H_A : \quad s = \mathcal{O}_p(n), q_\alpha = \mathcal{O}(\alpha^{-1}), \quad \Rightarrow \quad \mathbb{P}_{H_A}(s \geq q_\alpha) \rightarrow 1.$$

$$H_0 : \quad s = \mathcal{O}_p(1), q_\alpha = \mathcal{O}(\alpha^{-1}), \quad \Rightarrow \quad \mathbb{P}_{H_0}(s \geq q_\alpha) \rightarrow 0.$$

This ensures that

$$\lim_{n \rightarrow \infty} \mathbb{P}(|\hat{\mathcal{D}}| = |\mathcal{D}|) = 1.$$

From Lemma 3.2 of [Rice and Zhang \(2019\)](#), we know that

$$\arg \max_{\rho \in [\rho_0, \rho_1]} \lim_{l,r \rightarrow \infty} \left\| \frac{1}{\lceil (r-l)\rho \rceil} \sum_{i=l}^{l+\lceil (r-l)\rho \rceil} \mathbb{E}_{F^i} \phi(y) - \frac{1}{\lceil (r-l)(1-\rho) \rceil} \sum_{i=l+\lceil (r-l)\rho \rceil+1}^r \mathbb{E}_{F^i} \phi(y) \right\|^2 \in \{\rho_1^*, \dots, \rho_K^*\}.$$

Then from the uniform convergence of $T_1^{l,u}(t)$ and the argmax Theorem, we know that localization consistency holds.

For S_2 , notice that

$$T_2^{l,r}(t) \xrightarrow{p} \lim_{l,r \rightarrow \infty} \left| \frac{1}{t-l} \sum_{i=l}^t \mathbb{E}_{F^i} \|\phi(y_i) - \mathbb{E}_{F^i} \phi(y)\|^2 - \frac{1}{r-t} \sum_{i=t+1}^r \mathbb{E}_{F^i} \|\phi(y_i) - \mathbb{E}_{F^i} \phi(y)\|^2 \right| \text{ uniformly.}$$

Then, similar as for S_1 , the conclusion for S_2 follows directly. \square